Modulating Immune Regulation in Inflammatory Disease: Divergent Mechanisms in T Cell–Mediated Colitis and Regulatory T Cell Function

Von der Medizinischen Fakultät
der Rheinisch-Westfälischen Technischen Hochschule Aachen
zur Erlangung des akademischen Grades
eines Doktors der Theoretischen Medizin
genehmigte Dissertation

vorgelegt von

Sudheendra Hebbar Subramanyam, M.Sc.

aus

Anantapur (Indien)

Berichter: Prof. Dr. med. Klaus Tenbrock
Prof. Dr. rer. nat. Kim Ohl

Tag der mündlichen Prüfung: 15.06.2026

Diese Dissertation ist auf den Internetseiten der Universitätsbibliothek online verfügbar

To my parents, my wife, and my children, with deepest gratitude for their love and support

List of Publications

Dissertation

Hebbar Subramanyam S, Turyne Hriczko J, Schulz S, Look T, Goodarzi T, Clarner T, Scheld M, Kipp M, Verjans E, Böll S, Neullens C, Costa I, Li Z, Gan L, Denecke B, Schippers A, Floess S, Huehn J, Schmitt E, Bopp T, Wasmuth H, Winograd R, Beyaert R, Lambrecht B, Zenke M, Wagner N, Ohl K, Tenbrock K. CREB regulates Foxp3+ST-2+ TREGS with enhanced IL-10 production. Front Immunol. 2025 Jul 24; 16:1601008. doi: 10.3389/fimmu.2025.1601008.

Subramanyam SH, Hriczko JT, Pappas A, Schippers A, Wagner N, Ohl K, Tenbrock K. Tofacitinib fails to prevent T cell transfer colitis in mice but ameliorates disease activity. Sci Rep. 2023 Mar 7;13(1):3762. doi: 10.1038/s41598-023-30616-w.

Other publications

Hebbar Subramanyam S, Tenbrock K. Disarming a molecular brake: cAMP-responsive element modulator deletion supercharges CAR-NK cells. Sig Transduct Target Ther 10, 265 (2025). doi.org/10.1038/s41392-025-02362-0

Jong R, Rajendiran A, Hriczko JT, Subramanyam SH, Rein A, Häusler M, Orlikowsky T, Wagner N, Erny D, Ohl K, Tenbrock K. Human Genetic GLUT1 Deficiency Results in Impaired T Cellular IFN-γ Production. Eur J Immunol. 2025 Feb;55(2): e202451066. doi: 10.1002/eji.202451066.

Pappa A, Mührer J, Gast P, Hebbar Subramanyam S, Ohl K, Muschaweck M, Wagner N, Wenzl T, Tenbrock K. Pediatric IBD patients show medication and disease activity dependent changes in NK cell and CD4 memory T cell populations. Front Pediatr. 2023 Jun 29; 11:1123873. doi: 10.3389/fped.2023.1123873.

Rajendiran A, Subramanyam SH, Klemm P, Jankowski V, van Loosdregt J, Vastert B, Vollbach K, Wagner N, Tenbrock K, Ohl K. NRF2/Itaconate Axis Regulates Metabolism and Inflammatory Properties of T Cells in Children with JIA. Antioxidants (Basel). 2022 Dec 8;11(12):2426. doi: 10.3390/antiox11122426.

Subramanyam SH, Tenbrock K. The cAMP responsive element modulator (CREM) is a regulator of CD4+ T cell function. Biol Chem. 2021 Aug 26;402(12):1591-1596. doi: 10.1515/hsz-2021-0249.

Xu L, Liu L, Yao D, Zeng X, Zhang Y, Lai J, Zhong J, Zha X, Zheng R, Lu Y, Li M, Jin Z, Hebbar Subramanyam S, Chen S, Huang X, Li Y. PD-1 and TIGIT Are Highly Co-Expressed on CD8+ T Cells in AML Patient Bone Marrow. Front Oncol. 2021 Aug 18; 11:686156. doi: 10.3389/fonc.2021.686156.

Wynant N, Santos D, Subramanyam SH, Verlinden H, Vanden Broeck J. Drosha, Dicer-1 and Argonaute-1 in the desert locust: phylogenetic analyses, transcript profiling and regulation during phase transition and feeding. J Insect Physiol. 2015 Apr; 75:20-9. doi: 10.1016/j.jinsphys.2015.02.010.

frontiers | Frontiers in Immunology

TYPE Original Research
PUBLISHED 24 July 2025
DOI 10.3389/fimmu.2025.1601008

Check for updates

OPEN ACCESS

EDITED BY
Deborah Yablonski,
Technion Israel Institute of Technology, Israel

REVIEWED BY
Heth Roderick Turnquist,
University of Pittsburgh, United States
Wayne Hancock,
University of Pennsylvania, United States

*CORRESPONDENCE
Klaus Tenbrock
ktenbrock@ukaachen.de

†PRESENT ADDRESS
Martin Zenke,
Department of Medicine IV, Hematology, Oncology, and Stem Cell Transplantation, Rheinisch-Westfälische Technische Hochschule Aachen University Hospital, Aachen, Germany
Center for Integrated Oncology Aachen Bonn Cologne Duesseldorf (CIO ABCD), Aachen, Germany

‡These authors have contributed equally to this work

§Deceased

RECEIVED 27 March 2025
ACCEPTED 04 June 2025
PUBLISHED 24 July 2025
CORRECTED 29 August 2025

CITATION
Hebbar Subramanyam S, Turyne Hriczko J, Schulz S, Look T, Goodarzi T, Clarner T, Scheld M, Kipp M, Verjans E, Böll S, Neullens C, Costa I, Li Z, Gan L, Denecke B, Schippers A, Floess S, Huehn J, Schmitt E, Bopp T, Wasmuth H, Winograd R, Beyaert R, Lambrecht B, Zenke M, Wagner N, Ohl K and Tenbrock K (2025) CREB regulates Foxp3+ST-2+ T_{REGS} with enhanced IL-10 production. *Front. Immunol.* 16:1601008. doi: 10.3389/fimmu.2025.1601008

COPYRIGHT
© 2025 Hebbar Subramanyam, Turyne Hriczko, Schulz, Look, Goodarzi, Clarner, Scheld, Kipp, Verjans, Böll, Neullens, Costa, Li, Gan, Denecke, Schippers, Floess, Huehn, Schmitt, Bopp, Wasmuth, Winograd, Beyaert, Lambrecht, Zenke, Wagner, Ohl and Tenbrock. This is an open-access article distributed under the terms of the Creative Commons Attribution License (CC BY). The use, distribution or reproduction in other forums is permitted, provided the original author(s) and the copyright owner(s) are credited and that the original publication in this journal is cited, in accordance with accepted academic practice. No use, distribution or reproduction is permitted which does not comply with these terms.

CREB regulates Foxp3+ST-2+ T_{REGS} with enhanced IL-10 production

Sudheendra Hebbar Subramanyam[1], Judit Turyne Hriczko[1], Saskia Schulz[1], Thomas Look[2,3], Tannaz Goodarzi[1], Tim Clarner[4], Miriam Scheld[4], Markus Kipp[5], Eva Verjans[1], Svenja Böll[1], Christopher Neullens[1], Ivan Costa[6], Zhijian Li[6], Lin Gan[7], Bernd Denecke[7§], Angela Schippers[1], Stefan Floess[8], Jochen Huehn[8], Edgar Schmitt[9], Tobias Bopp[9], Hermann Wasmuth[10], Ron Winograd[10], Rudi Beyaert[11,12], Bart Lambrecht[11,13], Martin Zenke[2,3,14,15†], Norbert Wagner[1], Kim Ohl[1‡] and Klaus Tenbrock[1,16*‡]

[1]Department of Pediatrics, Rheinisch-Westfälische Technische Hochschule Aachen University Hospital, Aachen, Germany, [2]Helmholtz-Institute for Biomedical Engineering, Rheinisch-Westfälische Technische Hochschule Aachen University, Aachen, Germany, [3]Institute for Biomedical Engineering, Department of Cell Biology, Rheinisch-Westfälische Technische Hochschule Aachen University Hospital, Aachen, Germany, [4]Institute of Neuroanatomy and Jülich Aachen Research Alliance (JARA)-BRAIN, Faculty of Medicine, Rheinisch-Westfälische Technische Hochschule Aachen University, Aachen, Germany, [5]Institute of Anatomy, Medical University of Rostock, Rostock, Germany, [6]Instutute for Computational Genomics, Interdisciplinary Center for Clinical Research Aachen (IZKF Aachen), Rheinisch-Westfälische Technische Hochschule Aachen University Hospital, Aachen, Germany, [7]Genomics Facility, Interdisciplinary Center for Clinical Research Aachen (IZKF Aachen), Rheinisch-Westfälische Technische Hochschule Aachen University Hospital, Aachen, Germany, [8]Department of Experimental Immunology, Helmholtz Centre for Infection Research, Braunschweig, Germany, [9]Institute for Immunology, University Medical Center, Johannes Gutenberg University Mainz, Mainz, Germany, [10]Department of Medicine, Luiusenhospital Aachen, Aachen, Germany, [11]Vlaams Instituut voor Biotechnologie (VIB) Center for Inflammation Research, Ghent, Belgium, [12]Department of Biomedical Molecular Biology, Ghent University, Ghent, Belgium, [13]Department of Respiratory Medicine, Ghent University Hospital, Ghent, Belgium, [14]Department of Medicine IV, Hematology, Oncology, and Stem Cell Transplantation, Rheinisch-Westfälische Technische Hochschule Aachen University Hospital, Aachen, Germany, [15]Center for Integrated Oncology Aachen Bonn Cologne Duesseldorf (CIO ABCD), Aachen, Germany, [16]Division of Pediatric Rheumatology, Department of Pediatrics, Inselspital, Bern University Hospital, University of Bern, Bern, Switzerland

Introduction: Regulatory T-cells (T_{regs}) are characterized by the expression of Foxp3, a master regulator involved in the development and function of T_{regs}. Foxp3 expression is dependent on activity of the Treg specific demethylated site (TSDR), which contains a CREB binding site. We aimed to find out how Foxp3 specific CREB deletion affects Treg expression and function.

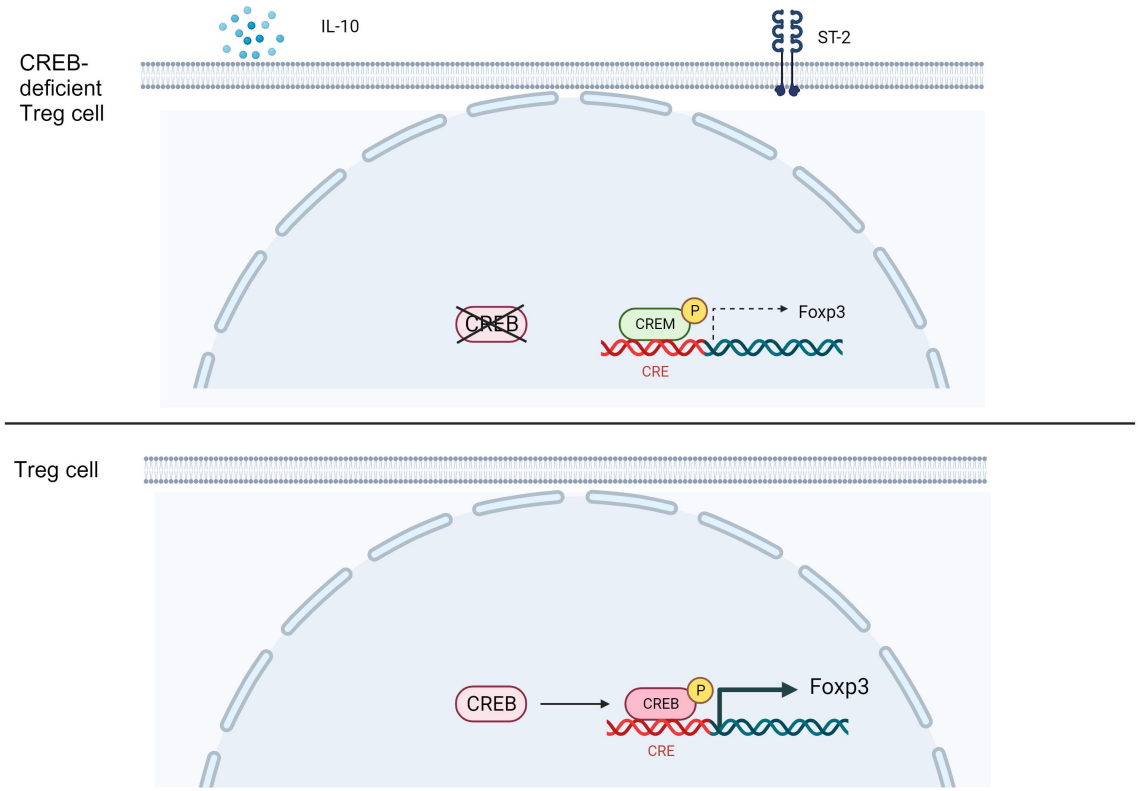
Methods: T_{regs} from *Foxp3^{cre}CREB$^{fl/fl}$* mice and wild type (*CREB$^{fl/fl}$*) mice were analyzed by flow cytometry. Cytokine analysis was performed by flow cytometry, ELISA and RT-qPCR. Gene expression analysis was performed using Affymetrix HTA2 assays, ATAC-sequencing, and Methylation-assays. For functional relevance, a CD4 T cell mediated transfer colitis was performed.

Results and discussion: *Foxp3^{cre}CREB$^{fl/fl}$* mice showed increased frequencies of T_{regs} (CD25+/Foxp3+) in thymus, spleen and peripheral lymph nodes and in

nonlymphoid organs including lung and colon, but decreased Foxp3 expression at the single cell level. Despite decreased Foxp3 expression, enhanced expression of the IL- 33 receptor (ST-2), IL-10, IL-13, and CREM was observed. CREB deficient T_{regs} were highly suppressive *in vitro* and prevented disease activity in a CD4 T cell mediated transfer colitis in an IL-10 dependent way. Mechanistically CREB fulfils dual roles in T_{regs}: (1) it promotes Foxp3 expression under Steady state conditions and (2) in cooperation with CREM, CREB restricts chromatin accessibility at the ST2 locus, thereby modulating IL-33 driven immune responses. This dual regulation balances FoxP3-dependent Treg stability with IL-10 mediated suppression of inflammation.

KEYWORDS

IL-33, ST2, Foxp3, IL-10, CREB, CREM



GRAPHICAL ABSTRACT

1 Introduction

Regulatory T cells (Tregs) marked by Foxp3 expression are important for immune balance. In the absence of Foxp3, mice (scurfy disease) (1) and humans (IPEX, polyglandular autoimmunopathy) develop severe autoimmune disease (2). Foxp3 Tregs arise from two sources; thymus-derived Tregs (t-Tregs) develop in the thymus, while inducible Tregs (iTregs) are generated in the periphery from conventional CD4+ T cells upon TGF-β stimulation (3). Both tT_{reg} and iT_{reg} generation largely depend on the presence of IL-2, which is not only required for homeostatic maintenance but also for the thymic development of T_{regs} (4–7).

ST-2, also known as IL1RL1, belongs to the Toll-like receptor/IL-1 receptor superfamily. ST-2, through its ligand IL-33, plays a pivotal role in MyD88/NFκB signaling. The interaction of ST-2 with its ligand IL-33 induces Foxp3 and GATA3 expression in T_{regs} at

mucosal sites (8). ST-2 mainly exists in two isoforms: soluble ST-2 (sST-2) and membrane-bound ST-2. sST-2 functions as a decoy receptor of IL-33 and inhibits NFκB signaling, while membrane-bound ST-2 promotes NFκB signaling (9). Increased ST-2 levels have been observed in diseases such as inflammatory bowel disease (IBD), asthma, colon cancers, and graft versus host disease (10). In many non-lymphoid tissues, T_{regs} show enriched expression of ST-2 and most of these are iT_{regs}. The regulation of ST-$2^{+}T_{regs}$ is dependent on the transcription factor basic leucine zipper transcription factor ATF-like (BATF) (11, 12), while other factors have not yet been defined. BATF belongs to the cAMP-responsive element binding protein/activating transcription factor (CREB/ATF) family of transcription factors, can dimerize with Jun, and has been shown to compete with CREB for binding to CRE/AP1 sites.

Our understanding of the molecular mechanism of suppression is still limited. IL-10 plays an important role in suppressing $CD4^{+}$ effector T-cell function. Additionally, IL-10 prevents activation of antigen-presenting cells (APCs), such as dendritic cells and macrophages, through the downregulation of costimulatory molecules and production of inflammatory cytokines within these cells (13). Selective ablation of IL-10 in $Foxp3^{+}$ T_{regs} revealed that IL-10 production by T_{regs} is essential for keeping the immune response in check at environmental interfaces such as the colon and lungs (14). IL-10 also acts in an autocrine manner by maintaining FoxP3 expression and the suppressive capacity of T_{regs} (15, 16). Interestingly, IL-10 is responsive to cAMP stimulation, at least in THP1 cells and macrophages, and the IL-10 promoter contains four putative cAMP response element sites (CRE, TGACGTCA), which are conserved between humans and mice (17). Following TLR activation, pCREB (phosphorylated CREB) is recruited to the IL-10 promoter and enhances IL-10 transcription in macrophages (18).

Previous data from Wang et al. (19) suggested that CREB negatively regulated the survival of iT_{regs} and is particularly important in the generation of CD4+Th17 cells. Using $CD4^{CRE}CREB^{fl/fl}$ mice, they showed that these cells prevented colitis in a $Rag2^{-/-}$ model; however, their model had the disadvantage that the CD4 cells of these mice expressed lower amounts of IL-2, which could have hampered iT_{reg} induction. Our analysis now expands upon their findings and determines an important role for CREB in the generation of ST2+T_{regs}. Using $Foxp3^{CRE}CREB^{fl/fl}$ mice, we herein confirm the colitis phenotype but can show that i) CREB deficiency in T_{regs} induces expression of ST2+T_{regs}, ii) the phenotype that prevents colitis in $Rag2^{-/-}$ mice is primarily dependent on abundance of IL-10, and iii) this phenotype can be reversed by knockout of CREM, which lowers the expression of ST2.

2 Materials and methods

2.1 Mouse strains

Experiments were performed with age-matched $CREB^{fl/fl}$, $VAV^{cre}CREB^{fl/fl}$, and $Foxp3^{cre}CREB^{fl/fl}$ mice (all C57BL/6). $Foxp3^{cre}CREB^{fl/fl}$ mice were generated by crossing CREB-flox mice (20) with C57BL/6 Foxp3-IRES Cre mice (provided by T. Bopp, University of Mainz, Germany). $Foxp3^{cre}$-$CREB^{fl/fl}$ mice were used as controls (denoted as $CREB^{fl/fl}$). $Foxp3^{Cre}ROSA^{RFP}$ mice were provided by T. Bopp University of Mainz and crossed with our $CREB^{fl/fl}$ mice. $Rag2^{-/-}$ (C57BL/6) mice were provided by A. Schippers (Uniklinik RWTH Aachen, Germany). All the mice were bred in our animal facility and kept under standardized conditions.

2.2 Transfer colitis

To induce transfer colitis, $Rag2^{-/-}$ mice were adoptively transferred 2 x 10^{6} $CD4^{+}$ $CD25^{-}$ T cells. Animals were sacrificed as soon as a significant loss of weight was measurable. The spleen and mesenteric lymph nodes (mLNs) were harvested for further analysis. One part of the colon was fixed in formalin for histological scoring and the other part was fixed in RNAlater (Qiagen, Germany) for subsequent mRNA analysis. For soluble ST2 (sST2) treatment, the mice received 100 µg mouse sST2 (produced by the VIB Protein Core facility, Belgium, and provided by R. Beyaert, VIB-UGent Center for Inflammation Research, Belgium), three times/week by intraperitoneal means (i.p). The control group received PBS i.p. For IL-10R treatment, the mice received 500 µg anti-IL-10R antibody (1B1mAB) (kindly provided by Prof. Edgar Schmitt, University of Mainz, Germany) or IgG control AK (Rat IgG kappa) i.p. once a week during the first 3 weeks.

2.3 Histological scoring

Initially, 4 µm paraffin sections from the fixed colon were cut serially, mounted onto glass slides, and deparaffinized. The colon sections were stained with hematoxylin and eosin by the Core Facility (IZKF) of the RWTH Aachen University. Blinded histological scoring was performed using a standard microscope, based on the JLS method as described previously (21, 22). Each colon section was scored for the four general criteria: severity, degree of hyperplasia, degree of ulceration, if present, and percentage of area involved. A subjective range of 1–3 (1 = mild, 2 = moderate, 3 = severe) was used for the first three categories. Severity: Focally small or widely separated multifocal areas of inflammation limited to the lamina propria were graded as mild lesions (1). Multifocal or locally extensive areas of inflammation extending to the submucosa were graded as moderate lesions (2). If the inflammation extended to all layers of the intestinal wall or the entire intestinal epithelium was destroyed, lesions were graded as severe (3). Hyperplasia: Mild hyperplasia consisted of morphologically normal lining epithelium that was at least twice as thick (length of crypts) as adjacent or control mucosa. Moderate hyperplasia was characterized by the lining epithelium being two or three times the normal thickness, cells were hyperchromatic, numbers of goblet cells were decreased, and scattered individual crypts developed an arborizing pattern. Severe hyperplastic regions

exhibited a markedly thickened epithelium (four or more times normal thickness), marked hyperchromasia of cells, few to no goblet cells, a high mitotic index of cells within the crypts, and numerous crypts with an arborizing pattern. Ulceration was graded as: 0 = no ulcer, 1 = 1–2 ulcers (involving up to a total of 20 crypts), 2 = 1–4 ulcers (involving a total of 20–40 crypts), and 3 = any ulcers exceeding the former in size. A 10% scale was used to estimate the area involved in the inflammatory process. 0 = 0%, 1 = 10%–30%, 2 = 40%–70%, 3 = >70%.

2.4 Cell isolation

Single cell suspensions were isolated from spleens and lymph nodes (LNs) [peripheral lymph nodes (pLNs) and mLNs] using cell strainers and erythrocytes were lysed with lysis buffer. To obtain immune cells from the lungs, tissue was excised into small pieces and digested with 0.1% collagenase in DPBS for 1hr. The digested fraction was passed through a 40µm nylon strainer and rinsed with DPBS. The flow through was centrifuged and the cell pellet was lysed using RBC lysis buffer. The cell pellet was used for the flow cytometric analysis. Colons were retrieved from the mice and rinsed with a cannula with PBS+0.5%BSA. Afterwards, the colons were excised into small pieces and placed in a digestive medium containing RPMI (10mL), collagenase V (0.85mg/mL), collagenase D (1.25mg/mL), dispase (1mg/mL) and DNase (30µg/mL) and incubated for 45 minutes at 37°C with gentle shaking. The digested fraction was passed through a 40 µm nylon strainer and the flow-through was collected and centrifuged to obtain a pellet. Percoll gradient centrifugation was performed by using 35% Percoll. The cell pellet obtained was lysed using RBC lysis buffer and was used for further analysis. The livers were retrieved from the mice. The gall bladders were removed and the livers were excised into small pieces and placed in a digestive medium containing RPMI without FCS (3mL), 1.25mg/mL collagenase D, and 30µg/mL DNase. The fraction was incubated for 45 minutes and digestion was stopped by adding PBS+0.5% BSA +2mM EDTA and homogenized using a syringe. The digested fraction was passed through a 100µm nylon strainer and the flow-through was centrifuged. The pellet obtained was used for the Percoll gradient centrifugation using 35% Percoll. The cell pellet obtained after the Percoll gradient centrifugation was lysed using RBC lysis buffer and was used for the flow cytometric analysis.

2.5 Suppression Assay

CD4 T-cells ($T_{effector}$ cells) were isolated from the spleens of wild-type mice. The cells were labeled with eFluor 660 proliferation dye from Thermo Fischer according to the manufacturer's instructions. After the labeling, the cells were stimulated with plate-coated anti-CD3 (10µg/mL, eBioscience, Germany) and soluble anti-CD28 (1µg/mL) (eBioscience) in the presence of CD4 +CD25+ cells from either wild-type or *Foxp3*^{cre}*CREB*$^{fl/fl}$ mice in different ratios (1:0, 1:0.5, 1:0.75, and 1:1) for 3 days. After 3 days of stimulation, the cells were analyzed using flow cytometric analysis.

2.6 T cell differentiation assays

Magnetic Activated Cell Sorting (MACS)-isolated $CD4^+CD25^-$ T cells ($2x10^6$ per mL) were incubated with plate-coated anti-CD3 (10µg/mL, eBioscience, Germany) and soluble anti-CD28 (1µg/mL) (eBioscience, Germany). T_H0 cells were left without exogenous cytokines, and 5 ng/mL TGF-β was added to induce T_{reg} differentiation.

2.7 Flow cytometry

For surface staining, single cell suspensions were stained with anti-CD4, anti-CD3, anti-CD8, anti-B220, anti-CD25, CD45, anti-GL-7, anti-ICOS, anti-ST2, anti-Nrp1, and anti-PD-1 (all from eBioscience, Germany). For intracellular staining of CREB, Foxp3, CTLA-4, Helios, GATA3, T-bet, and RORγt, cells were fixed and permeabilized with a FOXP3 staining buffer set (Thermo Fischer, eBioscience, Germany) following the manufacturer's instructions and stained with respective antibodies (eBioscience, Germany) for 30 min. Intracellular cytokines were stained with anti-IFN-γ-Alexa 647 (eBioscience, Germany) and anti-IL-17-Alexa 488 (BD, USA), and IL-10-APC (eBioscience, Germany) after PMA (30nM) and Ionomycin (1.5µM) (both Sigma-Aldrich, USA) re-stimulation in the presence of GolgiPlug/GolgiStop (BD Biosciences, USA). A daily calibrated FACS-Canto II flow cytometer (Becton Dickinson, MountainView, CA, USA) was used to perform the phenotypic analysis. Lymphocytes were gated by forward (FSC), side scatter (SSC), and CD3, CD4, and B220 expression. A figure exemplifying the gating strategies is provided in the Supplementary Materials (Supplementary Figure 6). For data analysis FCS-Express 4.0 Research Edition (DeNovo software Glendale, CA, USA) and FlowJo version 10 were used.

2.8 Luciferase assay

RLM cells carrying a stable pGL3-TSDR-FoxPro luciferase plasmid were kindly provided by Jochen Huehn (HZI Braunschweig, Germany). Cells were transfected with the pcDNA-CREB plasmid or pcDNA. Cells were left to rest overnight before luciferase activity was measured by using the Dual-Glo Luciferase Assay System (Promega, USA).

2.9 RNA isolation and real-time PCR

Total RNA from isolated T cells and colon tissue was isolated using the RNeasy Mini Kit (Qiagen, Germany). cDNA was then generated from 200 ng total RNA using the RevertAid H Minus First Strand cDNA Synthesis Kit (Thermo Fisher Scientific, USA) according to the manufacturer´s instructions. RT-PCR was performed using the SYBR Green PCR kit (Eurogentec, Germany) and data were acquired with the ABI Prism 7300 RT-PCR system (Applied Biosystems/Life Technologies, Germany). Each

measurement was set up in duplicate. After normalization to the endogenous reference control gene ß-actin for mice, the relative expression was calculated.

2.10 RNA extraction and microarray for gene expression analysis

$CD4^+CD25^+Nrp1^+$ T_{regs} were sorted by FACS. Genome-wide transcriptome analyses of $Foxp^{cre}CREB^{fl/fl}$ and $CREB^{fl/fl}$ T_{regs} were performed in independent triplicate using Gene Chip® Mouse Gene 2.0 arrays (Affymetrix, Santa Clara, CA, USA). Total RNA extraction was carried out using the RNeasy Micro Kit (Qiagen, Germany) according to the manufacturer's protocol and then quantified (Nanodrop). RNA quality was assessed using the RNA 6000 Nano Assay with the 2100 Bioanalyzer (Agilent, Santa Clara, CA, USA). Samples for the Gene 2.0 arrays were prepared and hybridized to the arrays according to the Affymetrix WT Plus Kit manual. Briefly, for each sample, 100 ng of total RNA was reverse-transcribed into cDNA using a random hexamer oligonucleotide tagged with a T7 promoter sequence. After second-strand synthesis, double-strand cDNA was used as a template for amplification with T7 RNA polymerase to obtain antisense cRNA. Random hexamers and dNTPs spiked out with dUTP were then used to reverse-transcribe the cRNA into single-stranded sense-strand cDNA. The cDNA was then fragmented with uracil DNA glycosylase and apurinic/apyrimidic endonuclease 1. The fragment size was checked using the 2100 Bioanalyzer and ranged from 50 to 200 bp. Fragmented sense cDNA was biotin-end-labeled with TdT and the probes were hybridized to the Gene 2.0 arrays at 45°C for 16h with 60 rpms. Hybridized arrays were washed and stained on a Fluidics Station 450 (program: FS450 0002) and scanned on a GeneChip® Scanner 3000 7G (both Affymetrix). Raw image data were analyzed with Affymetrix® Expression Console™ Software (Affymetrix, USA), and gene expression intensities were normalized and summarized with a robust multiarray average algorithm (23). Transcripts that were expressed differently more than 1.5-fold with a raw p-value lower than 0.05 between the sample groups were categorized as regulated. A enrichment analysis for Wiki pathways was performed using WebGestalt (24). For the enrichment analysis only, genes that changed at least 1.5-fold with a p-value lower than 0.05 between $Foxp3^{cre}CREB^{fl/fl}$ and $CREB^{fl/fl}$ samples were taken into consideration.

2.11 TSDR methylation analysis

For all the methylation analyses, cells from male mice were used. Genomic DNA was prepared from FACS-sorted T_{conv} cells ($CD4^+CD25^-$) and T_{reg} cells ($CD4^+CD25^+Nrp1^+$) from $CREB^{fl/fl}$ and $Foxp3^{cre}CREB^{fl/fl}$ mice and subsequently converted by bisulfite according to the manufacturer's instructions (DNeasy Blood & Tissue Kit, Qiagen; EZ DNA Methylation-Lightning Kit, Zymo Research, USA). Pyrosequencing of the Treg cell-specific demethylated region (TSDR) (chromosome position X:7583950-7584149, genome assembly GRCm38.p6) was performed as described previously (25).

2.12 Transposase-accessible chromatin assay using sequencing

Omni-transposase-accessible chromatin assay using sequencing (ATAC-seq) was performed according to (26, 27) with minor modifications. Prior to transposition, dead cells were removed by centrifugation (800 rpm, 4 min, 4°C). The transposition reaction was conducted with 7.5 µL Tagment DNA Enzyme 1 (TDE1) for 60 min at 37°C. Pre-amplification was conducted with NEBNext Ultra II Q5 Master Mix and Nextera PCR Primers (5 cycles). Quantitative PCR amplification was conducted with NEBNext Ultra II Q5 Master Mix, Nextera PCR Primer, and SYBR Gold to determine the number of additional cycles. PCR amplification of additional cycles was the same as for pre-amplification. PCR fragments were purified with Qiagen MinElute PCR Purification Kit and library concentration and quality were determined using an Agilent High Sensitive DNA Kit and TapeStation, respectively. ATACseq libraries were sequenced on the Illumina NextSeq 500 Platform with 75 bps paired-end reads in duplicate. ATAC-seq libraries were trimmed with Trim Galore (parameters -q 30 –paired –trim1) and aligned to the mouse genome (mm9) using Bowtie2 (28) (parameters -X2000 –no-mixed –no-discordant). Duplicate fragments were removed, and reads were filtered for alignment quality of >Q30 using samtools (29). Next, we used MAC2 (30) to perform peak calling (parameters: nomodel, nolambda, keep-dup auto, call-summits). Transcription factor footprinting and differential activity was performed using HINT-ATAC as described in Li et al. (27).

2.13 ELISA

Total IgG and IgE were measured from sera using the Ready-Set-Go ELISA system (affymetrix: eBioscience, USA). IL-10 was determined in cell supernatants using mouse IL-10 ELISA Ready-SET-GO! (2nd Generation) (Thermo Fisher Scientific, USA), according to the manufacturer's instructions.

2.14 Statistical analysis

All data are presented as mean ± standard error (SEM). Data were tested for normality using the Shapiro–Wilk normality test. Differences between two groups were evaluated using two-tailed unpaired or paired (if indicated) Student's t-tests. A two-tailed Mann–Whitney test was used if data were not normally distributed. One-way ANOVA was performed if there are more than two groups. Measurements were taken from distinct samples. All statistical analysis and subsequent graphics generation were performed using GraphPad Prism versions 7.0 and 8.0 (GraphPad Software, USA). A p-value <0.05 was statistically significant.

2.15 Study approval

The animal study was approved by the regional government authorities and animal procedures were performed according to German legislation for animal protection. Permission for the projects was granted by the Regierungspräsident/LANUV Nordrhein-Westfalen (81-02.04. 2017.A393).

2.16 Data availability

The ATAC-Seq and microarray raw datasets have been deposited in GEO under the accession codes GSE157693 and GSE157933. All data that support the findings of this study are available within the article and the Supplementary Material. All other data, including raw data used in each figure, will be provided upon reasonable request to the corresponding author.

3 Results

3.1 CREB enhances T_{reg} numbers but downregulates Foxp3 expression in T_{regs}

CREB is a transcriptional activator and has been found to critically stabilize Foxp3 expression (31). It is therefore widely accepted that CREB promotes FoxP3 expression in T_{regs} (32–34). To verify this hypothesis *in vivo*, we generated mice with a Foxp3-specific knockout of CREB (*Foxp3*^{cre}*CREB*$^{fl/fl}$). To our surprise, these mice showed enhanced numbers of CD25$^+$/Foxp3$^+$ positive T_{regs} in the thymus (Figures 1A, D), spleen (Figures 1B, D), and pLN (Figures 1C, D). Splenic T_{regs} showed no altered expression of Nrp1, PD-1, CTLA4, and ICOS (Supplementary Figures 1A, B). There was also no convincing different expression of T_h lineage transcription factors GATA3 and RORγT and T-bet in CD4$^+$Foxp3$^+$ cells within different organs (Supplementary Figures 2A–E). However, *Foxp3*^{cre}*CREB*$^{fl/fl}$ mice displayed lower Foxp3 expression in T_{regs} on the single cell level (Figures 1E, F), which can be explained by the fact that CREB directly activates the TSDR (31) (Figure 1G). To verify Cre expression in the Foxp3-Cre mice, we crossed *Foxp3*^{cre}*CREB*$^{fl/fl}$ mice with Cre-inducible reporter mice (*ROSA*^{RFP}) and examined reporter gene expression in lymphocytes. RFP expression was confined to CD4$^+$CD25$^+$ cells, which is important for excluding cell extrinsic side-effects (Figures 1H, I).

We further used *Foxp3*^{cre}*CREB*$^{fl/fl}$ *ROSA*^{RFP} mice to assess the percentages of T_{regs} in non-lymphoid organs. While we did not observe differences in liver tissue, we found a particularly marked upregulation of T_{reg} percentages within the lungs and colons of *Foxp3*^{cre}*CREB*$^{fl/fl}$ *ROSA*^{RFP} mice compared to *Foxp3*^{cre}*ROSA*^{RFP} mice (Figures 1J–L) and enhanced absolute numbers of T_{regs} in the colons of Foxp3^{cre}*CREB*$^{fl/fl}$ *ROSA*^{RFP} (Supplementary Figure 7B). This prompted us to analyze whether CREB expression in T_{regs} differs in different tissues. We could not find an association between high tissue-dependent CREB expression and the effects of CREB deficiency on T_{reg} percentages; however, we found a high expression of CREB in murine colonic T_{regs} (Supplementary Figure 8).

3.2 CREB-deficient T_{regs} are suppressive *in vitro*

To test whether lower Foxp3 expression affects the suppressive capacity of CREB-deficient T_{regs}, we co-cultured *CREB*$^{fl/fl}$ T_{regs} and *Foxp3*^{cre}*CREB*$^{fl/fl}$ T_{regs} with anti-CD3 and anti-CD28 stimulated WT CD4$^+$ cells. Surprisingly, *Foxp3*^{cre}*CREB*$^{fl/fl}$ T_{regs} revealed an increased capacity to reduce CD4$^+$ T cell proliferation (Figures 2A, B). These data suggest that deletion of CREB, despite reducing Foxp3 expression per cell, enhances the function of T_{regs}. In addition, the expression of Helios was enhanced (Figure 2C) and bisulfite sequencing revealed a demethylated TSDR (Figure 2D), which suggests a stable and suppressive phenotype (35). In conclusion, despite the reduction of Foxp3 levels per cell, CREB deficiency leads to stable and functional T_{regs} *in vitro*.

3.3 CREB-deficient T_{regs} reveal gene expression signature with enhanced expression of IL-10, IL-4, IL-13, and ST2

To understand why CREB-deficient T_{regs} are suppressive despite reduced Foxp3 expression, we performed a whole transcriptome analysis (Affymetrix HTA2 arrays) of flow-sorted (CD4$^+$CD25$^+$Nrp-1$^+$) *Foxp3*^{cre}*CREB*$^{fl/fl}$ and *CREB*$^{fl/fl}$ T_{regs} (Supplementary Figure 3A) and appropriate wild-type mice because, at the time of this analysis, the *Foxp3*^{CRE}*CREB*$^{fl/fl}$ *ROSA*^{RFP} mice were not yet available. Using a fold-change of 1.5 and a p-value of less than 0.05, we found 111 downregulated and 122 upregulated genes in the *Foxp3*^{cre}*CREB*$^{fl/fl}$ compared to the *CREB*$^{fl/fl}$ T_{regs}, and among them, IL-10 and IL-13 were the two most differentially regulated in the *Foxp3*^{cre}*CREB*$^{fl/fl}$ T_{regs} (Figure 3A). KEGG pathway analysis revealed an enrichment of differentially regulated genes in pathways that are associated with Th2 cytokines, such as asthma, Th2 and Th2 cell differentiation, and cytokine-cytokine receptor interaction pathways (Figure 3B). Higher *Il13* and *Il10* mRNA expression in *Foxp3*^{cre}*CREB*$^{fl/fl}$ T_{regs} could be further confirmed by RT-qPCR (Figures 3C, D). CD4$^+$CD25$^+$Foxp3$^+$ cells also showed enhanced IL-10 protein levels after 3 days of CD3/CD28 stimulation, as assessed by flow cytometry (Figures 3E, F). *In vitro* T_{reg} differentiation with TGF-β revealed a reduced capacity of *Foxp3*^{cre}*CREB*$^{fl/fl}$ T cells to differentiate towards Foxp3$^+$ cells, while IL-10 expressing cells within Foxp3$^+$ cells were enhanced (Figure 3G). Furthermore, IL-10 cytokine expression of TGF-β–stimulated *Foxp3*^{cre}*CREB*$^{fl/fl}$ T cells measured by ELISA was enhanced, as was *Il13, Il5*, and *Il10* mRNA expression, which suggests that CREB deficiency in T_{regs} induces a Th2-biased phenotype (Figures 3H-L). Beyond cytokines, Il1r1 (ST2) showed enhanced expression on the microarray. ST2, the receptor of IL-33, is preferentially expressed on colonic T_{regs}, where it promotes T_{reg} function and adaptation to the inflammatory environment. It provides a necessary signal for T_{reg}-cell

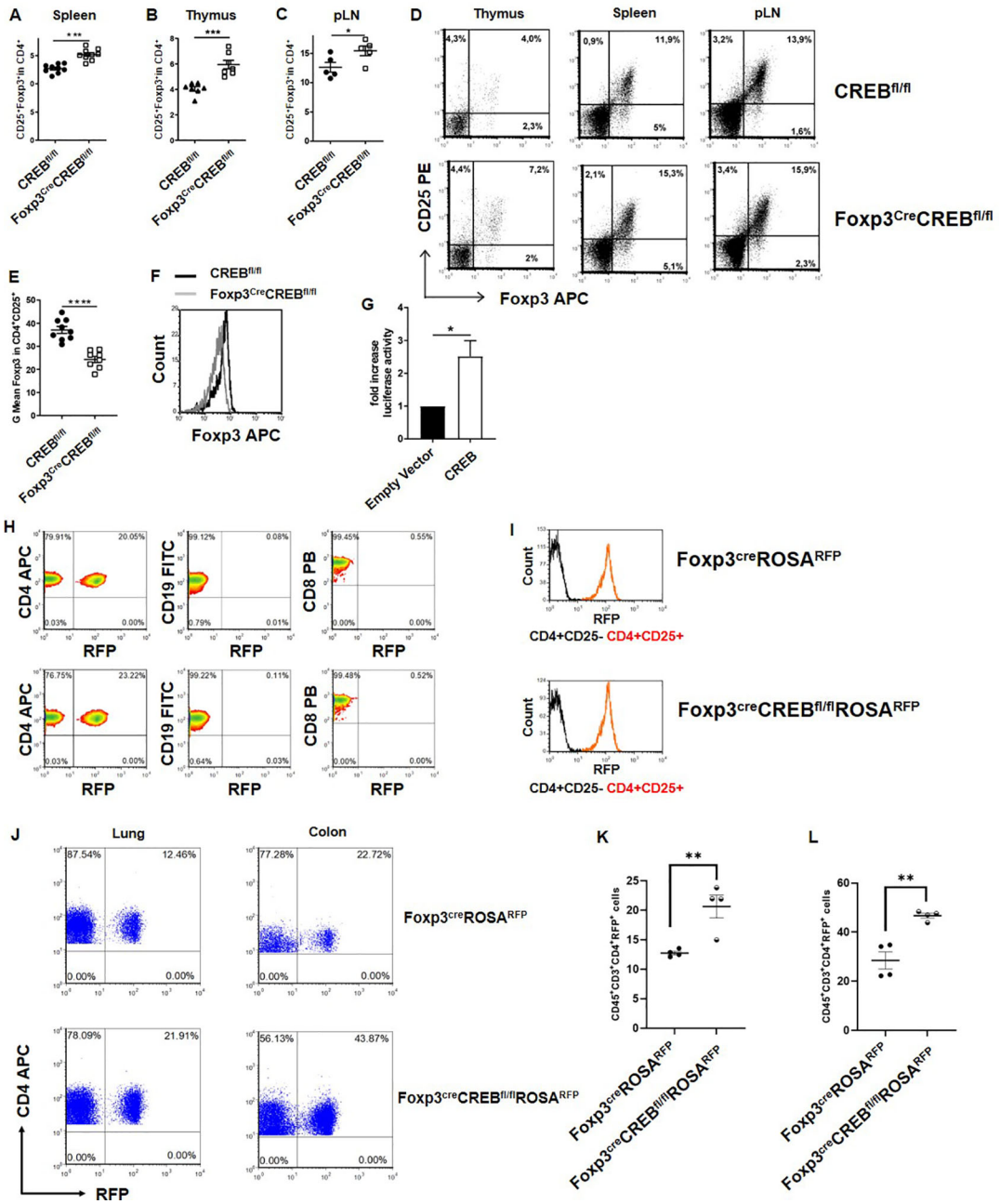


FIGURE 1
Genetic deletion of CREB in Foxp3$^+$ cells increases the percentage of T_{regs} but downregulates their Foxp3 expression. **(A)** Statistical analysis of splenic T_{reg} ($CD4^+CD25^+Foxp3^+$) percentages from *CREB$^{fl/fl}$* and *Foxp3^{cre}CREB$^{fl/fl}$* mice (N = 9, four independently performed experiments, each with 2–3 age and sex-matched mice that were 6–9 weeks old). **(B)** Statistical analysis of T_{reg} percentages within the thymuses ($CD3^+CD4^{sp}CD25^+Foxp3^+$) of *CREB$^{fl/fl}$* and *Foxp3^{cre}CREB$^{fl/f\ l}$* mice ($N$ = 7, three independently performed experiments, each with 2–3 age and sex-matched mice that were 6–9 weeks old). **(C)** Statistical analysis of T_{reg} ($CD4^+CD25^+Foxp3^+$) percentages from pLNs of *CREB$^{fl/fl}$* and *Foxp3^{CRE}CREB$^{fl/fl}$* mice (N =5, two independently performed experiments, each with 2–3 age and sex-matched mice that were 7–9 weeks old). **(D)** Density plot showing $CD25^+Foxp3^+$ cells gated on $CD3^+CD4^+CD8^-$ cells in the thymuses of *CREB$^{fl/fl}$* and *Foxp3^{cre}CREB$^{fl/fl}$* mice (left), $CD25^+Foxp3^+$ cells gated on $CD4^+$ cells in the spleens of *CREB$^{fl/fl}$* and *Foxp3^{cre}CREB$^{fl/fl}$* mice (middle), and $CD4^+CD25^+$Foxp3+ cells in the pLNs from *CREB$^{fl/fl}$* and *Foxp3^{cre}CREB$^{fl/fl}$* mice (right). **(E)** Statistical analysis of mean fluorescent intensity (MFI) of Foxp3 in *CREB$^{fl/fl}$* and *Foxp3^{cre}CREB$^{fl/fl}$* $CD4^+CD25^+$ T cells (N=6, 3 independently performed experiments, each with two animals that were 6–8 weeks old and sex- and age-matched). **(F)** Representative histogram showing an overlay of Foxp3 expression in $CD4^+CD25^+$ cells from *CREB$^{fl/f\ l}$*(black) and *Foxp3^{cre}CREB$^{fl/fl}$* (grey) spleens. **(G)** RLM cells carrying a stable pGL3-TSDR-FoxPro luciferase plasmid were transfected either with an empty vector or CREB plasmid and stimulated with PMA, and luciferase activity was measured after 4 hours (N = 5). **(H)** Percentages of RFP^+ cells within the $CD4^+$ (on the left), $CD19^+$ (in the middle), and $CD8^+$ populations (on the right) in the spleens of *Foxp3^{cre}ROSA^{RFP}* and *Foxp3^{cre}CREB$^{fl/fl}$ROSA^{RFP}* mice. **(I)** Representative histogram showing the MFI of RFP expression in $CD4^+CD25^-$ (black) and $CD4^+CD25^+$ cells (red) in the spleens of *Foxp3^{cre}ROSA^{RFP}* and *Foxp3^{cre}CREB$^{fl/fl}$ROSA^{RFP}* mice. **(J)** Percentage of RFP^+ cells within the $CD45^+CD3^+CD4^+$ population in the lungs and colons of *Foxp3^{cre}ROSA^{RFP}* and *Foxp3^{cre}CREB$^{fl/fl}$ROSA^{RFP}* mice. **(K)** Statistical analysis of $CD45^+CD3^+CD4^+RFP^+$ cells in the lung tissue of *Foxp3^{CRE}ROSA^{RFP}* and *Foxp3^{cre}CREB$^{fl/fl}$ROSA^{RFP}* mice (N=4, three independently performed experiments). **(L)** Statistical analysis of $CD45^+CD3^+CD4^+RFP^+$ cells in the colon tissue of *Foxp3^{cre}ROSA^{RFP}* and *Foxp3^{cre}CREB$^{fl/fl}$ROSA^{RFP}* mice (N=4, three independently performed experiments). Two-tailed, unpaired t-tests were used to test the significance. *p<0.05, **p<0.01, ***p<0.001, and ****p<0.0001 and the results are expressed as the mean ± SEM.

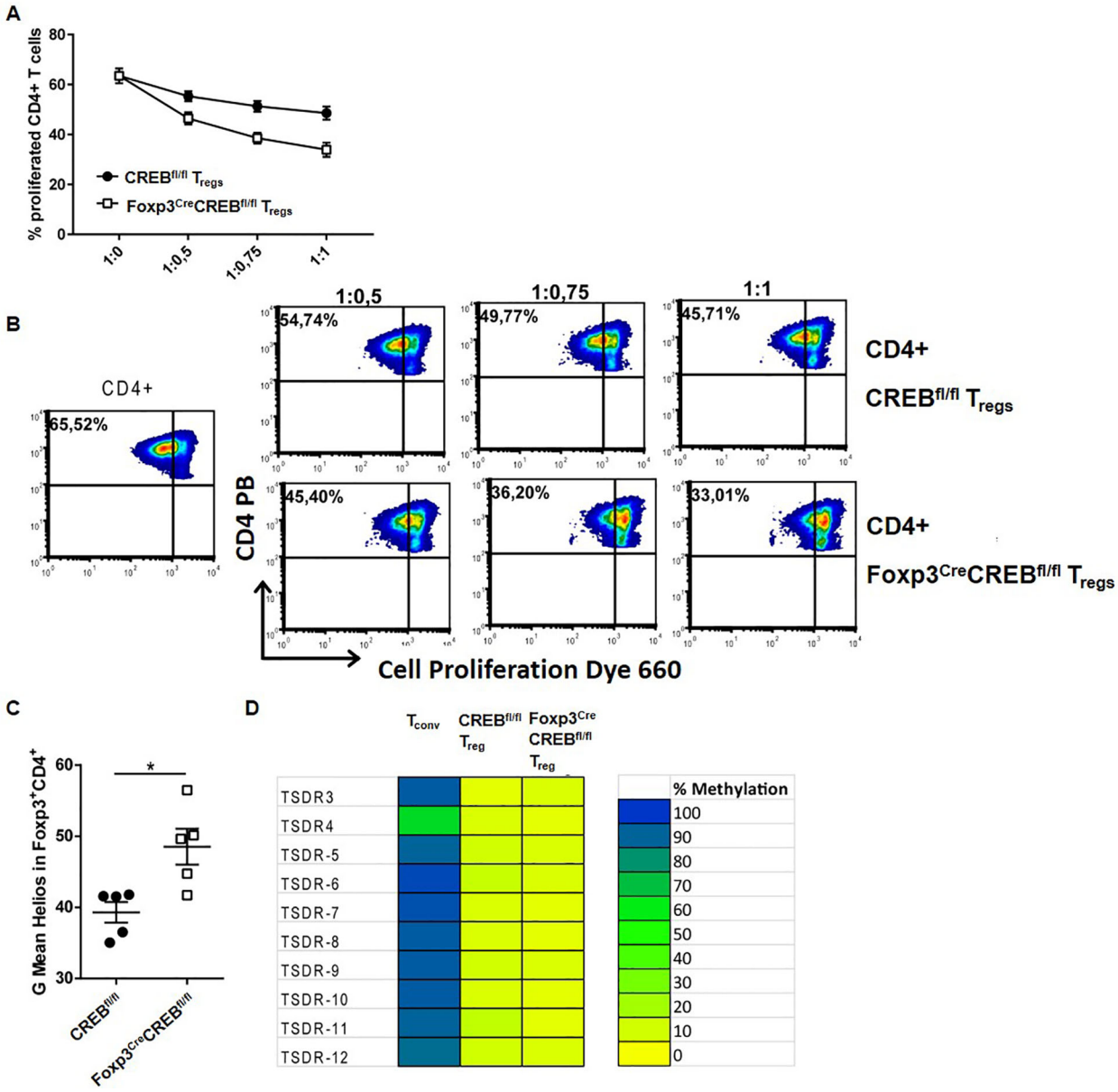


FIGURE 2
In vitro suppressive capacity of T_{regs} is enhanced in the absence of CREB. **(A)** WT $CD4^+$ T cells from the spleens (T_{eff}) were labeled with eFluor 660 and stimulated with anti-CD3/CD28 antibodies for 3 days. $CD4^+CD25^+$ T cells (T_{regs}) from *CREB*$^{fl/fl}$ or *Foxp3*^{cre}*CREB*$^{fl/fl}$ animals were added in different ratios (1:0, 1:0.5, 1:0.75, and 1:1). The proliferation of responder T cells was assessed in a eFluor 660 (eBioscience) dilution (*N = 3*) using flow cytometry **(B)** Representative density plots of **(A)**. **(C)** Statistical analysis of MFI of helios in *CREB*$^{fl/fl}$ and Foxp3^{cre}*CREB*$^{fl/fl}$ $CD4^+Foxp3^+$ T cells (*N = 5*, 2 independently performed experiments, each with 2–3 animals that were 8 weeks old and sex-matched; a two-tailed Mann–Whitney test was performed to test for significance). **(D)** Representative TSDR methylation patterns of purified $CD4^+CD25^+Nrp1^+$ T_{reg} cells and $CD4^+CD25^-$ conventional T cells isolated from the spleens of 6–8-week-old male mice (*N = 4*). Amplicons are vertically arranged, each representing a single CpG motif. The methylation rate of each motif was translated into a yellow-green-blue color code. *p<0.05, and all the results are expressed as the mean ± SEM.

accumulation and maintenance in inflamed tissues, and it was shown to regulate IL-10-expressing T_{regs} in the gut (8). In addition, IL-33 has been identified as a major interleukin in asthma pathology (36). ST2 was highly expressed in the *Foxp3*^{cre}*CREB*$^{fl/fl}$ T_{regs}, which was confirmed by flow cytometry (Figures 3M, N). Moreover, the whole transcriptome analysis also revealed an upregulated expression of CREM in *Foxp3*^{cre}*CREB*$^{fl/fl}$ T_{regs} and qRT-PCR also showed tendentially enhanced CREM expression in *Foxp3*^{cre}*CREB*$^{fl/fl}$ T_{regs} (Figure 3O). In conclusion, these data suggest that CREB deletion induces $ST2^+$ T_{regs}. This finding led us to investigate the protein expression of ST2 within different organs in *Foxp3*^{cre}*ROSA*^{RFP} and *Foxp3*^{cre}*CREB*$^{fl/fl}$*ROSA*^{RFP} mice. ST2 expression was clearly enhanced in T_{regs} in the thymus, spleens, mesenteric lymph nodes, lungs, and colons of these mice (Figures 3P–T).

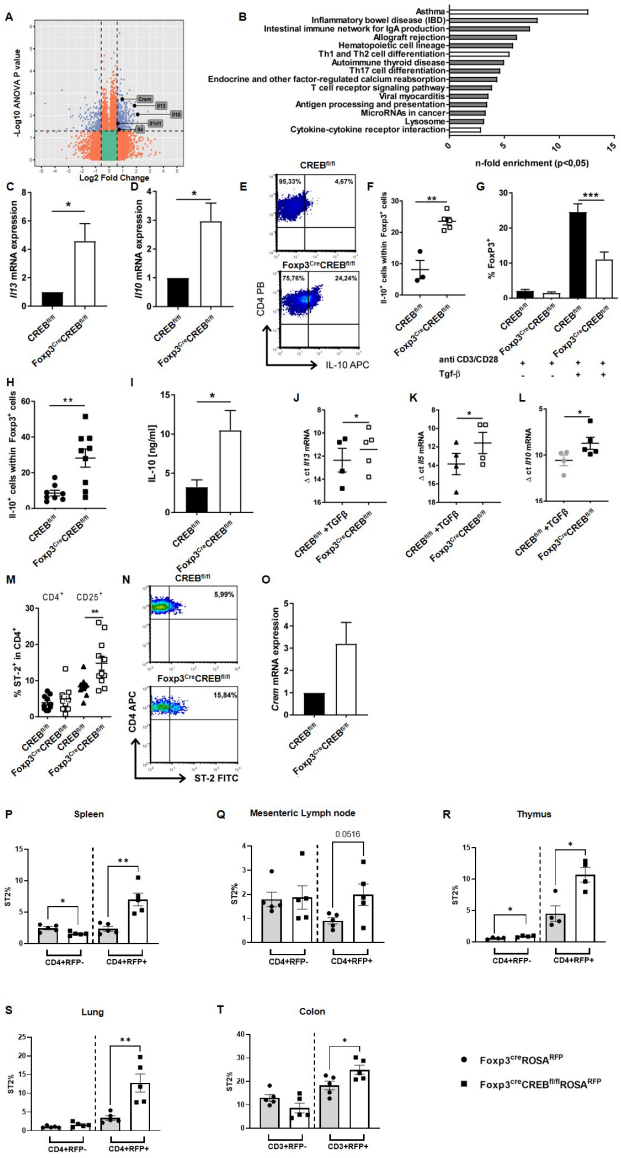


FIGURE 3
Altered gene expression in CREB deficient T_{regs}. **(A)**Gene expression in T_{regs} from the spleens of *CREB*$^{fl/fl}$ and *Foxp3*^{cre}*CREB*$^{fl/fl}$ mice. Colors indicate significant upregulation or downregulation of at least 1.5-fold with a p-value not more than 0.05 (blue); regulation of at least 1.5-fold or regulation with p-value not more than 0.05 (red). **(B)** Selection of pathways and associated genes that were significantly enriched. **(C)** N-fold *Il13* mRNA expression in splenic T_{regs} from *CREB*$^{fl/fl}$ and *Foxp3*^{cre}*CREB*$^{fl/fl}$ mice (*N = 5*, male, 8–10 weeks old) analyzed by RT-qPCR. Bars indicate the mean and error bars the SEM, and a two-tailed one-sample test was used to test for significance. **D)** N-fold *Il10* mRNA expression in splenic T_{regs} from *CREB*$^{fl/fl}$ and *Foxp3*^{cre}*CREB*$^{fl/fl}$ mice (*N = 5*, male, 8–10 weeks old) analyzed by RT-qPCR. Bars indicate mean and error bars SEM, and a two-tailed one-sample test was used to test for significance. **E)** MACS-isolated T cells from spleens were stimulated *ex vivo* with anti-CD3/CD28 antibodies for 3 days and re-stimulated with PMA/Ionomycin in the presence of Golgi Plug™. A representative density plot shows IL-10 production in CD4$^+$Foxp3$^+$ cells. **(F)** Statistical analysis of IL-10 expression of Foxp3$^+$ cells after treatment as in **(E)** (*N = 3* independent experiments, each dot represents one animal, two tailed unpaired t-test. **(G)** CD4$^+$CD25$^-$ T cells were stimulated with anti-CD3/CD28 antibodies in the presence/absence of 5 ng/mL TGF-β for 5 days. Percentages of Foxp3$^+$ cells from six independently performed experiments were determined, each with the spleen from one mouse (*N =13 CREB*$^{fl/fl}$ and *N=12 Foxp3*^{cre}*CREB*$^{fl/fl}$ mice), and a two-tailed unpaired t-test was used to test for significance. **(H)** Statistical analysis of IL-10$^+$ cells within Foxp3$^+$ cells after treatment as in G). An unpaired two-tailed t-test was used to test for significance, each dot represents one animal, and error bars the SEM. **(I)** IL-10 in supernatants of CD4$^+$CD25$^-$ T cells after stimulation with anti-CD3/CD28 antibodies in the presence of 5 ng/mL TGF-β for 5 days was measured by ELISA, and an unpaired two- tailed t-test was performed to test for significance. The bars indicate the mean and the error bars the SEM (*N = 6*). **(J–L)** Δ ct mRNA expression of cells after treatment as in **(G)** Each dot represents one animal and error bars the SEM. Two-tailed unpaired t-tests were used to test for significance. **(M)** Statistical analysis of splenic ST2$^+$ cells within CD4$^+$ and CD4$^+$CD25$^+$ cells of *CREB*$^{fl/fl}$ and *Foxp3*^{cre}*CREB*$^{fl/fl}$ mice. There were three independently performed experiments (*N = 10 CREB*$^{fl/fl}$ and *N =11 Foxp3*^{cre}*CREB*$^{fl/fl}$ mice), a two-tailed unpaired t-test was used to test for significance, and each dot represents one animal and error bars the SEM. **(N)** Representative density plot of M. **(O)** N-fold *Crem* mRNA expression in splenic T_{regs} from *CREB*$^{fl/fl}$ and *Foxp3*^{cre}*CREB*$^{fl/fl}$ mice (N = 3, male, 8–10 weeks old) cells analyzed by RT-qPCR. **(P–T)** Statistical analysis of ST2$^+$ in CD4+ and CD4+RFP+ cells in *Foxp3*^{cre}*ROSA*^{RFP} (*N = 5*) and *Foxp3*^{cre}*CREB*$^{fl/fl}$*ROSA*^{RFP} (N = 5) in the **(P)** spleens, **(Q)** mesenteric lymph nodes, **(R)** thymuses, and **(S)** lungs. Bars indicate mean and error bars the SEM, and a two-tailed unpaired t-test was used to test for significance. **(T)** Statistical analysis of ST2+ in CD3+ and CD3+RFP+ cells in *Foxp3*^{cre}*ROSA*^{RFP} (*N = 5*) and *Foxp3*^{cre}*CREB*$^{fl/fl}$*ROSA*^{RFP} (*N = 5*) in the colon. A two-tailed unpaired t-test was used to test for significance. *p<0.05, **p<0.01, and ***p<0.001, and the results are expressed as the mean ± SEM.

3.4 *Foxp3*^{cre}*CREB*$^{fl/fl}$ T cells dampen inflammation in experimental colitis

Since ST2^{+}T$_{regs}$ also play a protective role in intestinal mucosal inflammation (8), we performed a transfer of *Foxp3*^{cre}*CREB*$^{fl/fl}$ T cells (CD4+CD25-) or appropriate *CREB*$^{fl/fl}$ T cells (CD4+CD25-) into lymphopenic Rag2$^{-/-}$ mice. This usually results in the development of colitis within 5 weeks. Strikingly, the transfer of *Foxp3*^{cre}*CREB*$^{fl/fl}$ T cells did not result in the expected weight loss (Figure 4A) and the recipient mice displayed decreased intestinal inflammation (Figures 4B, C). Furthermore, there was a significant decrease of *Il6, Tnfa, Il17a*, and *Ifng*, along with a non-significant trend towards decreased *Il1b* in the

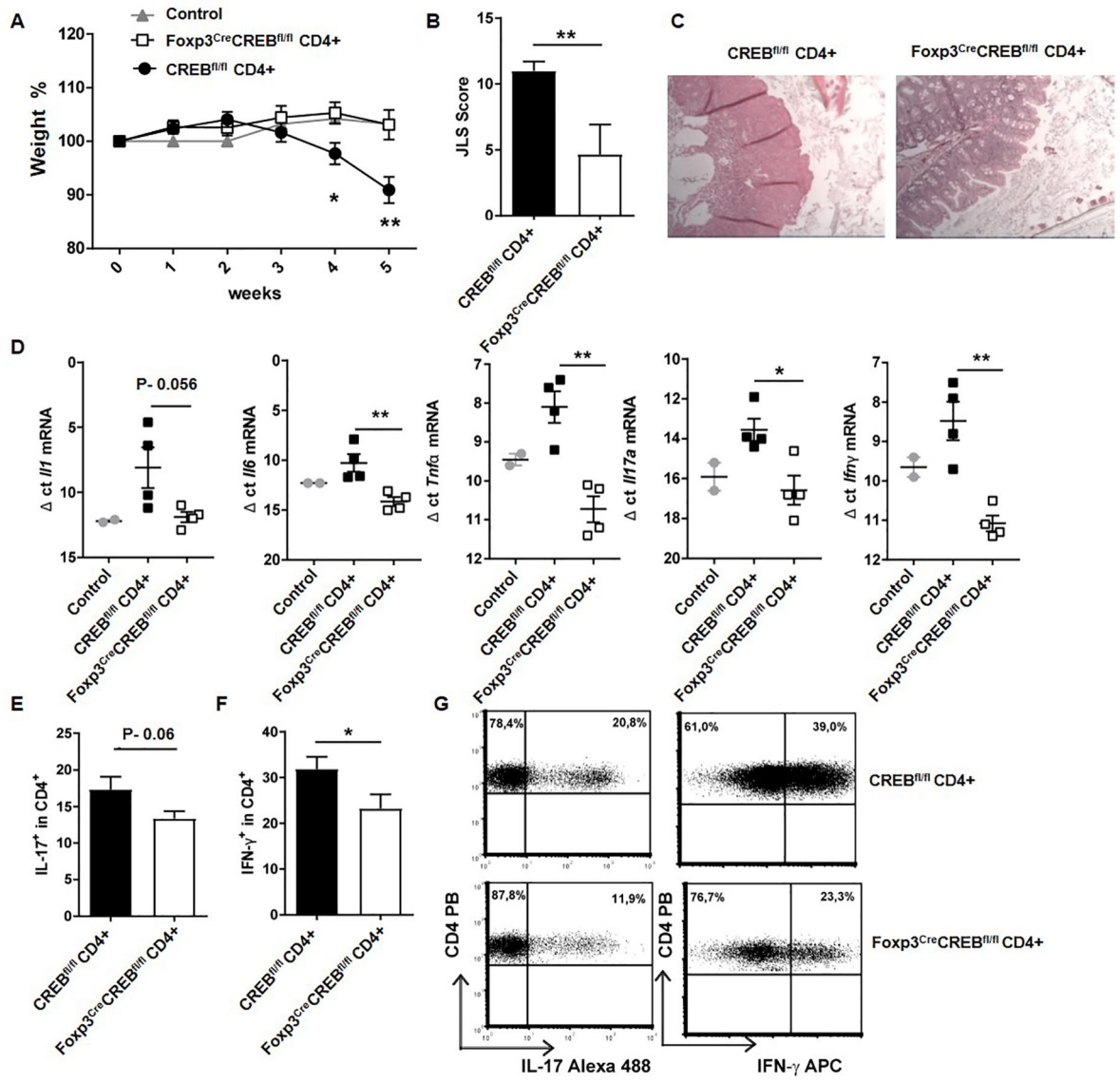


FIGURE 4
Foxp3^{cre}*CREB*$^{fl/fl}$ CD4+ T cells induce only moderate inflammation in experimental colitis. Rag2$^{-/-}$ mice were adoptively transferred CD4^{+} CD25^{-} wild-type cells (*CREB*$^{fl/fl}$ CD4^{+}) or *Foxp3*^{cre}*CREB*$^{fl/fl}$ CD4^{+} CD25^{-} T cells. Untreated Rag$^{-/-}$ mice were used as controls. Mice were weighed and sacrificed 5 weeks after transfer. **(A)** Body weight as a percentage of starting weight. A two-tailed unpaired t-test were used to test for significance (*N = 11 CREB*$^{fl/fl}$, *N = 9 Foxp3*^{cre}*CREB*$^{fl/fl}$ recipients, and five control Rag$^{-/-}$ mice were analyzed in three independently performed experiments). **(B)** Results of histological JLS score of colon sections (two independently performed experiments; *CREB*$^{fl/fl}$ recipients N = 5, *Foxp3*^{cre}*CREB*$_{fl/fl}$ recipients N = 6; a two-tailed Mann–Whitney test was used). **(C)** Representative photomicrographs of H&E-stained colon sections imaged using 10x magnification. **(D)** Expression of inflammatory cytokines analyzed by RT-qPCR. Dots represent Δ ct values normalized to β-actin. Each dot represents one animal (ct levels are inversely proportional to the amount of target nucleic acid in the sample). Two-tailed unpaired t-tests were used to test for significance (*N = 2* control mice, *N = 4 CREB*$^{fl/f}$, *N = 4 Foxp3*^{cre}*CREB*$^{fl/fl}$ recipients). **(E)** Statistical analysis of IL-17^{+} cells within CD4^{+} cells in mLNs (three independently performed experiments, *CREB*$^{fl/fl}$ recipients N = 9, *Foxp3*^{cre}*CREB*$^{fl/fl}$ recipients N = 9). A two-tailed unpaired t-test was used. **(F)** Statistical analysis of IFN-γ^{+} cells within CD4^{+} cells in mLNs (Three independently performed experiments; *CREB*$^{fl/fl}$ recipients *N = 11*, *Foxp3*^{cre}*CREB*$^{fl/fl}$ recipients *N = 9*). A two-tailed unpaired t-test was used. **(G)** Representative dot plots of E and **(F)** *p<0.05 and **p<0.01 and the results are expressed as the mean ± SEM.

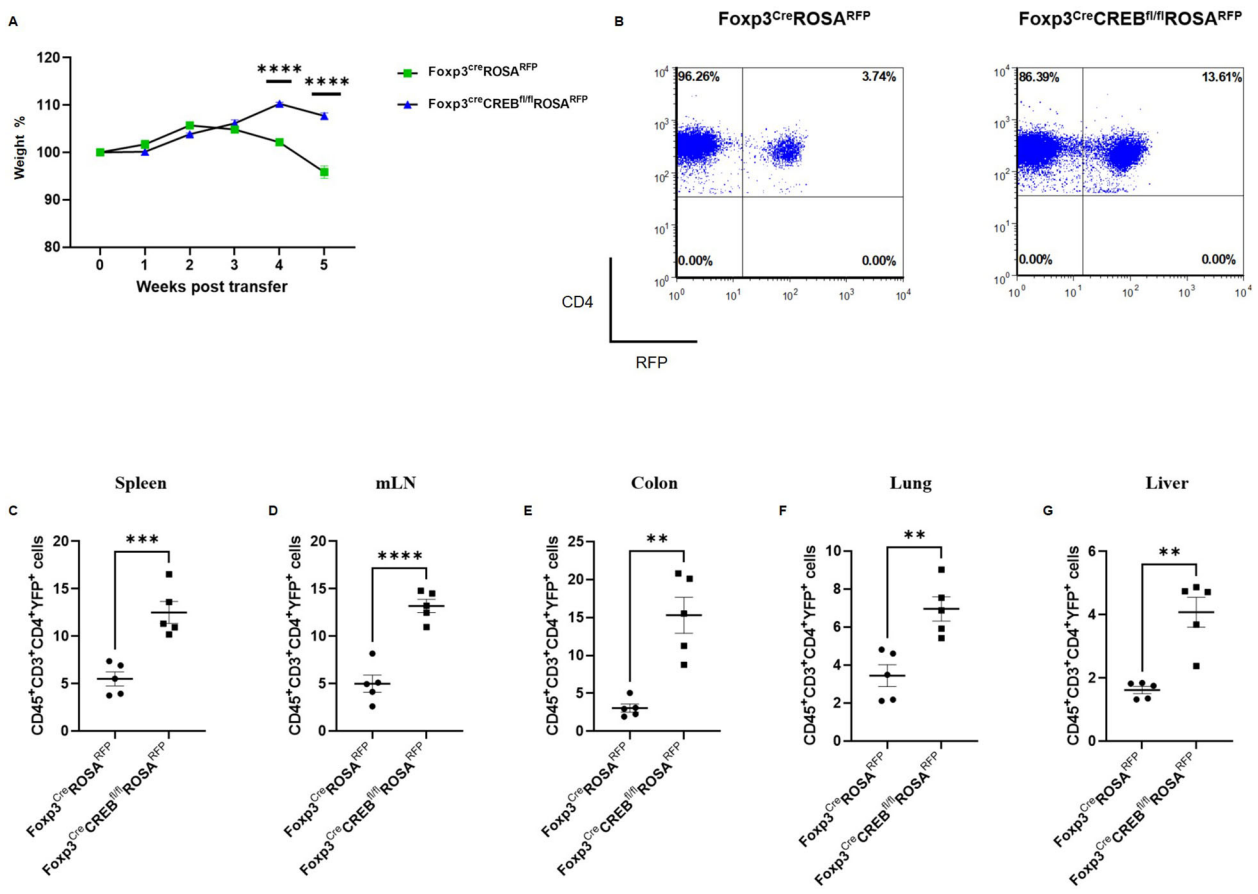


FIGURE 5
Foxp3^{cre}*CREB*$^{fl/fl}$*ROSA*^{RFP} CD4+ T cells induce only moderate inflammation in experimental colitis, while CD4+RFP+ cells expand in peripheral tissues. Rag2$^{-/-}$ mice were adoptively transferred CD4^{+} CD25^{-} wild-type cells (*Foxp*^{cre}*ROSA*^{RFP}CD4^{+}) or *Foxp3*^{cre}*CREB*$^{fl/fl}$*ROSA*^{RFP} CD4^{+} CD25^{-} T cells. Mice were weighed and sacrificed 5 weeks after transfer. **(A)** Body weight as a percentage of starting weight. A two-tailed unpaired t-test was used to test for significance (*N = 5 Foxp*^{cre}*ROSA*^{RFP} and *N = 5 Foxp3*^{cre}*CREB*$^{fl/fl}$*ROSA*^{RFP} recipient mice were analyzed in one independently performed experiment). B) Dot plots representing frequencies of RFP^{+} cells within the CD45^{+}CD3^{+}CD4^{+} population in the spleens of Rag2-/- mice that received cells from either *Foxp3*^{cre}*ROSA*^{RFP} or *Foxp3*^{cre}*CREB*$^{fl/fl}$*ROSA*^{RFP} mice. Percentages of CD45^{+}CD3^{+}CD4^{+}RFP^{+} cells in the **(C)** spleens, **(D)** mLNs, **(E)** colons, **(F)** lungs, and **(G)** livers. A two-tailed unpaired t-test was used. **p<0.01, ***p<0.001, and ****p<0.0001 and the results are expressed as the mean ± SEM.

gut (Figure 4D) and reduced IFN-γ production. There was also a trend towards reduced IL-17A in CD4^{+} T cells in the mLNs (Supplementary Figure S4E–G). Limitations include the absence of IL-6 and TNFα protein data due to the limited availability of the tissue. The experiment was repeated with CD4+CD25- T cells from *Foxp3*^{cre}*ROSA*^{RFP} and *Foxp3*^{cre}*CREB*$^{fl/fl}$ *ROSA*^{RFP} mice into Rag2-/- mice and with CD4 +CD25- cells from *CREB*$^{fl/fl}$ *and VAV*^{cre}*CREB*$^{fl/fl}$ mice into Rag2-/- mice, with the same results. The transfer of CD4+CD25- T cells from *Foxp3*^{cre}*CREB*$^{fl/fl}$ *ROSA*^{RFP} mice (Figures 5A–G) and from *VAV*^{cre}*CREB*$^{fl/fl}$ prevented the development of colitis (Supplementary Figure 11) and resulted in enhanced accumulation of RFP+ T_{regs} in different organs (Figures 5A–G). Interestingly, RFP+ T_{regs} also accumulated in the liver, while we did not find a difference in the RFP expression in the *Foxp3*^{cre}*CREB*$^{fl/fl}$ *ROSA*^{RFP} mice under steady state conditions.

3.5 Blockade of IL-10 but not of ST2 signaling reverses the protective effects of *Foxp3*^{cre}*CREB*$^{fl/fl}$ T cells in experimental colitis

ST2^{+} T_{regs} are protective in intestinal inflammation (8), and,in addition, they are Th_2 biased and release IL-10 (37). To decipher whether *Foxp3*^{cre}*CREB*$^{fl/fl}$ T cells prevent colitis through IL-10 production and/or ST2 expression, we performed an adoptive transfer colitis experiment with anti-IL10R antibodies or recombinant soluble ST2 (sST2). sST2 acts as a decoy for IL-33 and inhibits its biological activity (38). The blockade of IL-10 signaling induced colitis in the formerly resistant *Foxp3*^{cre}*CREB*$^{fl/fl}$ T cell-recipient mice (Figures 6A–C), while the ST2 blockade had no effect on disease progression (Supplementary Figure 4).

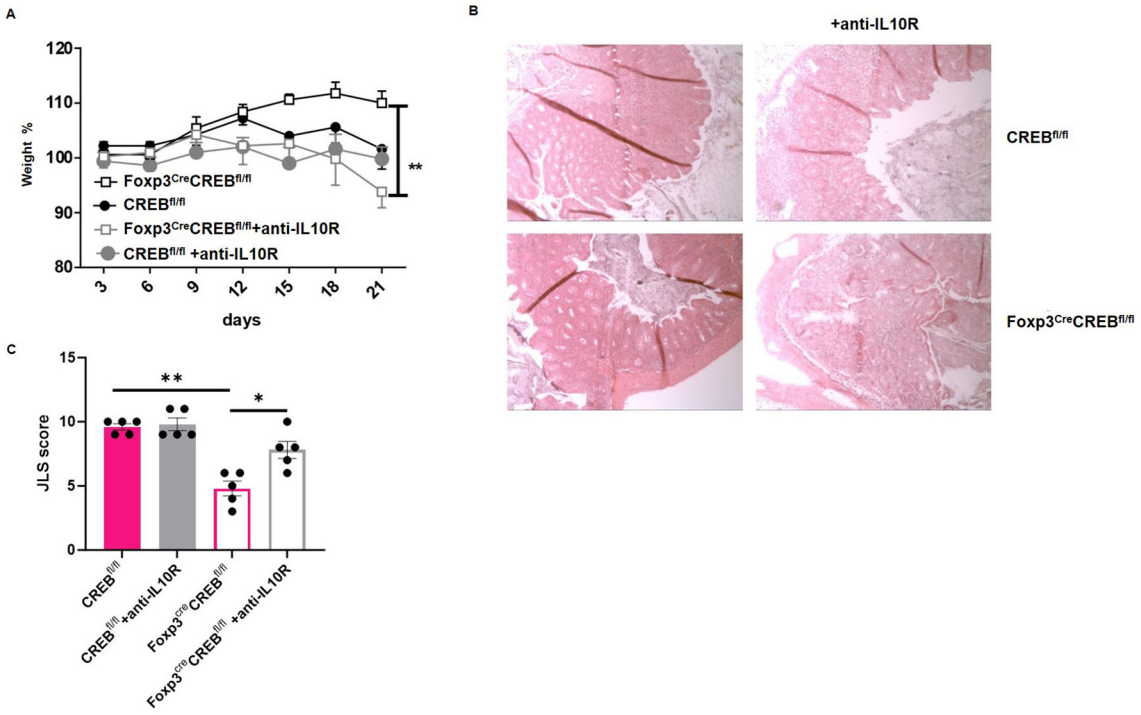


FIGURE 6
Reduced colitis in *Foxp3*^{cre}*CREB*$^{fl/fl}$ CD4$^+$ T cell recipients depends on IL-10 signaling. Rag2$^{-/-}$ mice were adoptively transferred CD4$^+$ wild-type cells (WT CD4$^+$) or *Foxp3*^{cre}*CREB*$^{fl/fl}$ CD4$^+$ T cells. Mice were either treated with an anti-IL10R antibody or an isotype control. **(A)** Body weight as a percentage of starting weight. Bars indicate mean and error bars the SEM (*N=5* animals in each group; a two-tailed unpaired t-test was used; two independently performed experiments). **(B)** Representative photomicrographs of a H&E-stained colon section from *CREB*$^{fl/fl}$ and *Foxp3*^{cre}*CREB*$^{fl/fl}$ CD4$^+$ T cell recipients that were treated with anti-IL10R, imaged using 10x magnification. **(C)** Results of histological JLS score of colon sections (two independently performed experiments with overall *N=5* mice in each group; a two-tailed Mann–Whitney test was used to test for significance). *p<0.05 and **p<0.01 and the results are expressed as the mean ± SEM.

3.6 Genome-wide chromatin accessibility of WT and CREB-deficient T_{regs}

To analyze whether CREB deletion alters chromatin accessibility at different promoters and enhancers, we performed ATAC-seq in *CREB*$^{fl/fl}$ and *Foxp3*^{cre}*CREB*$^{fl/fl}$ T_{regs}. We observed a decrease in open chromatin around CREB and CREM motifs in the *Foxp3*^{cre}*CREB*$^{fl/fl}$ mice, which indicates loss of binding activity of these transcription factors in these cells (Figure 7A). The *Il1rl1* (ST2) region showed significant differences in open chromatin around the original and an alternative promoter in T_{regs} from the *Foxp3*^{cre}*CREB*$^{fl/fl}$ mice, while canonical CRE motifs, which are 8-base pair palindromic sequences (5′-TGACGTCA-3′), could not be identified (Figure 7B). In addition, the IL-10 enhancer region showed clear differences between the two mouse strains. Within this region, binding sites for Nrf1 were identified, which is a CREB-dependent transcription factor (39). Moreover, we found a change in open chromatin of an alternate promoter of CREM (Figure 7C). CREM has been identified as one of the most regulated genes in ST-2 positive colonic T_{regs} of healthy mice (40). To prove whether CREM is involved in the regulation of ST2, we generated *Foxp3*^{cre}*CREB*$^{fl/fl}$*CREM*$^{-/-}$ mice. *In vitro* differentiation towards Foxp3+ cells was not significantly diminished in *Foxp3*^{cre}*CREB*$^{fl/fl}$*CREM*$^{-/-}$ mice (Figure 7D). Furthermore, deletion of CREM normalized Foxp3 expression per cell in CREB-deficient T_{regs} at least to some extent (Figure 7E) but reversed the expression of ST2 (Figure 7F). Taken together, our data suggest that the interaction of CREB and CREM determines the expression of Foxp3 and ST2 and the induction of CREM in CREB-deficient T_{regs} contributes to reduced Foxp3 expression. To prove the effect *in vivo*, we performed a transfer of *Foxp3*^{cre}*CREB*$^{fl/fl}$CREM$^{-/-}$ T cells (CD4+CD25-) or appropriate wild-type T cells (CD4+CD25-) into lymphopenic Rag2$^{-/-}$ mice. The additional genetic deletion of CREM reversed the effect of the CREB deletion and resulted in enhanced colitis severity, measured by JLS (The Jackson Laboratory Scoring) score in the transferred mice (Figure 7G).

4 Discussion

In this study, we provide evidence that CREB cells intrinsically regulate Foxp3 expression in T_{regs} and thereby play a critical role in T_{reg} cell-mediated immune homeostasis. In detail, CREB deficient T_{regs} showed a reduced expression of Foxp3 per cell but enhanced expression of ST2, IL-10, and IL-13. Enhanced IL-10 expression of CREB-deficient T_{regs} prevents T cell-mediated colitis. Enhanced IL-10 expression is also a hallmark of ST2$^+$ T_{regs}. ST2 is expressed on colonic T_{regs} and enhances local intestinal T_{reg} cell responses (8).

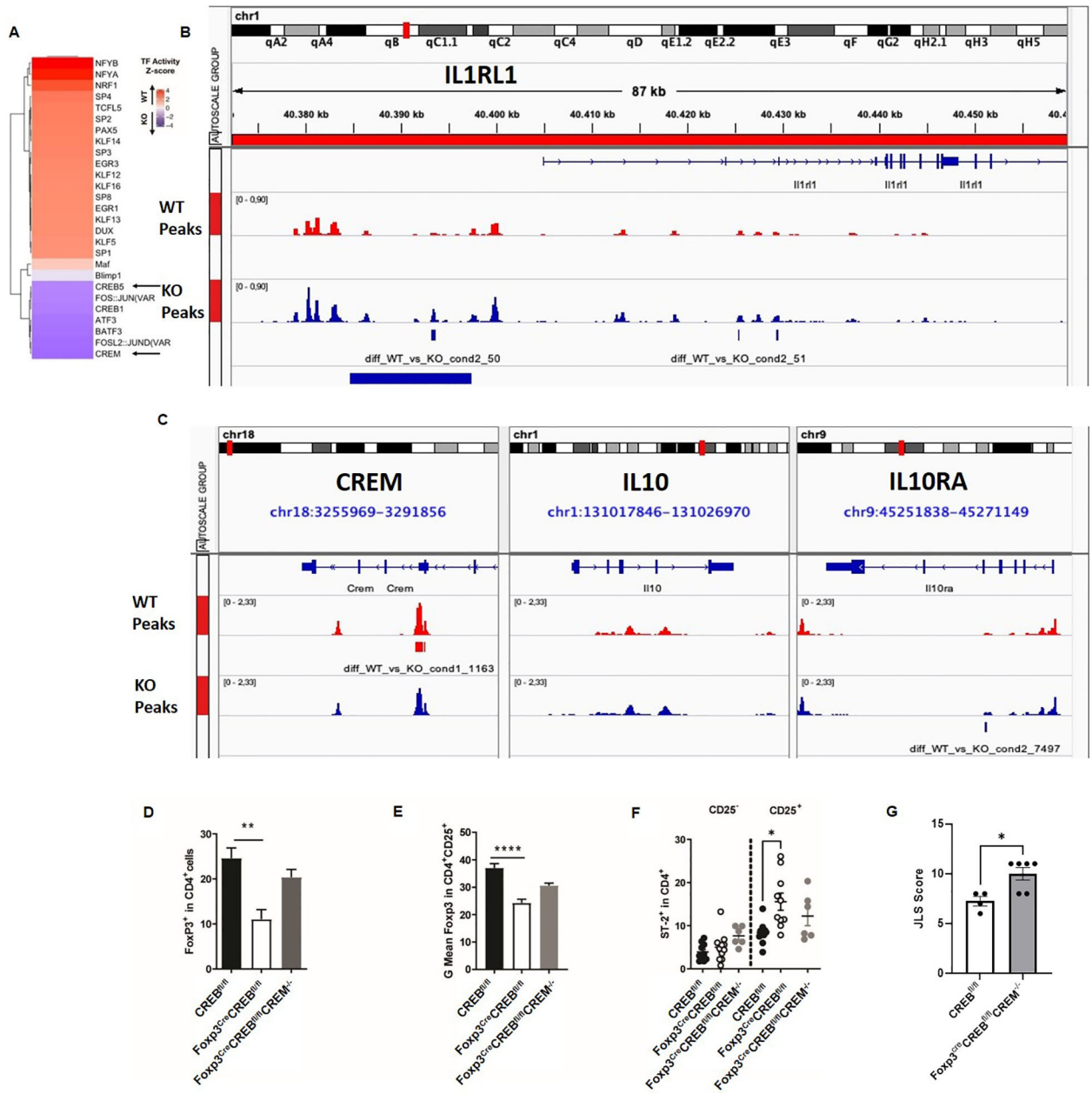


FIGURE 7
Genome-wide chromatin accessibility of *CREB*$^{fl/fl}$ and *Foxp3*^{cre}*CREB*$^{fl/fl}$ mice. **(A)** ATAC-seq foot printing analysis indicates a decrease in TF activity for CREB and CREM upon CREB KO and an increase in TF activity of NRF1 upon CREB KO (p-value < 0.05; z-test). **(B, C)** Example of genes with loss of chromatin accessibility upon CREB KO includes enhancer regions around SC-2/Il1rl1 (blue peaks) and an alternative promoter of CREM (red peaks) (adjusted p-value < 0.05; MACS2 diff. peak caller). **(D)** CD4$^+$CD25$^-$ T cells were stimulated with anti-CD3/CD28 antibodies in the presence/absence of 5 ng/mL TGF-β for 5 days. Percentages of Foxp3$^+$ cells from six independently performed experiments were determined, each with the spleen from one mouse (*N* = 13 *CREB*$^{fl/fl}$, *N* = 12 *Foxp3*^{cre}*CREB*$^{fl/fl}$, and *N* = 3 *Foxp3*^{cre}*CREB*$^{fl/fl}$*CREM*$^{-/-}$ mice; a two-tailed unpaired t-test was used to test for significance; bars indicate the mean and error bars the SEM). **(E)** Statistical analysis of MFI of Foxp3 in *CREB*$^{fl/fl}$ (*N* = 13), *Foxp3*^{cre}*CREB*$^{fl/fl}$ (N = 9), and *Foxp3*^{cre}*CREB*$^{fl/fl}$*CREM*$^{-/-}$ (*N* =3) CD4$^+$CD25$^+$ T cells. Bars indicate the mean and error bars the SEM, and a two-tailed unpaired t-test was used to test for significance. **(F)** Statistical analysis of ST2$^+$ in CD4$^+$ and CD4$^+$CD25$^+$ cells in *CREB*$^{fl/fl}$ (*N* = 5), *Foxp3*^{cre}*CREB*$^{fl/fl}$ (*N* = 6), and *Foxp3*^{cre}*CREB*$^{fl/fl}$*CREM*$^{-/-}$ (*N* =3) CD4$^+$CD25$^+$ T cells. Bars indicate the mean and error bars the SEM, and one-way ANOVA was used to test for significance. **(G)** Rag2$^{-/-}$ mice were adoptively transferred *CREB*$^{fl/fl}$ CD4 T-cells (CD4$^+$CD25-) or *Foxp3*^{cre}*CREB*$^{fl/fl}$ CREM$^{-/-}$ CD4$^+$ T cells (CD4+CD25-). Histological JLS score results of the colon sections (one experiment with overall *N=4/5* mice in each group; a two-tailed Mann–Whitney test was used to test for significance). *p<0.05, **p<0.01, and ****p<0.0001 and the results are expressed as the mean ± SEM.

We identified particularly enhanced expression of T_{regs} in the colons and lungs of *Foxp3*^{cre}*CREB*$^{fl/fl}$ mice, which also includes upregulation of ST2 expression and may contribute to the unexpectedly protective role of CREB deletion in T_{regs} in type I immune responses. This protective role is in line with Wang et al. (19) who demonstrated an important role for CREB in regulating the balance between Th17 cells and T_{regs}. They showed that mice bearing a deletion of CREB in all CD4$^+$ T cells prevented T cell-

mediated transfer colitis comparable to our model. Moreover, these mice were also resistant in an EAE model. This protective effect in EAE was surprisingly lost when CREB was specifically deleted in T_{regs}. Nevertheless, except in the EAE model, Wang et al. did not analyze the Foxp3-specific CREB-deleted mice in further detail.

We hypothesize that, in particular, the enhanced IL-10 secretion prevented colitis in Rag-/- mice that received *Foxp3*^{cre}*CREB*$^{fl/fl}$ CD4+ T cells. IL-10 is an important regulator of intestinal homeostasis, as IL-10 and IL-10R deficient mice spontaneously develop intestinal inflammation (41, 42) and blocking IL-10 signaling induced colitis in *Foxp3*^{cre}*CREB*$^{fl/fl}$ T cell recipients that were previously resistant. It has been shown before that CREB induces IL-10 transcription in macrophages. Our data, thus, were highly unexpected and do not support these findings but may instead argue for cell-dependent mechanisms that regulate IL-10 expression. Our ATAC-seq data however do not show a direct effect of CREB expression on chromatin accessibility within the IL-10 enhancer and promoter region, thus we currently cannot mechanistically explain these findings.

We also found enhanced percentages of T_{regs} within the thymus, spleens, and pLNs but reduced Foxp3 expression per cell within peripheral lymphoid organs. Wang et al. also suggest that compensation by related transcription factors such as CREM exist. Interestingly and corroborating that theory, we found a clear upregulation of CREM in CREB-deficient T_{regs} and additional deletion of CREM recuperates Foxp3 expression in CREB deficient T_{reg} cells, while it downregulates ST2 expression. Strikingly, CREM expression, which was enhanced in *Foxp3*^{cre}*CREB*$^{fl/fl}$ T_{regs}, was found before as a highly regulated gene in ST2-positive colon and skin T_{regs} (40). Delacher et al. characterized ST2$^+$ tissue T_{regs} that are present in all non-lymphoid tissues, which were found to express killer cell lectin-like receptor subfamily G1 (KLRG1) and Th2-associated factors, including IL-10 (11, 12). These "tisT_{regs}ST-2" cells are programmed by BATF (12) in lymphoid organs and perform important tissue homeostasis and regenerative functions. Our data point to the fact that the expression of CREB and CREM also regulate these tisT_{reg}ST2 in non-lymphoid tissues such as the colon, lungs, and liver. Spath et al. vigorously analyzed ST2 trajectories in mice and showed a high plasticity in ST2 expression and hierarchies in tissue-specific phenotypes (43). In addition, they found that ST2$^+$ T_{regs} were highly proliferative and had a high migratory potential. This is in line with our findings that these cells can be found in the spleen, lung, liver, mLN, and the colon. They additionally found a high prevalence in skin and VAT, which was not analyzed in our setting. When comparing the transcriptional profiles with our analyses, we can confirm an upregulation of PTPN13 in our data (1.97-fold) and a regulation of Rab4a (-1.51-fold) between the CREB-deficient T_{regs} and wild-type T_{regs}, and the other factors that distinguished ST2$^+$ from ST2$^-$ T_{regs} (Lyn, Gata3, Rln3, Klrg1, and Tbc1d4) were not different. Interestingly, in their analysis, ST2$^+$ T_{regs} were enriched in more activated, differentiated T_{reg} populations, such as ID2$^+$ T_{regs}, and ID2 was upregulated in our analysis as well (1.7-fold) (43).

The limitations of our study are that we mainly mechanistically analyzed splenic T_{regs}, while ST2 is a hallmark of tissue T_{regs}, and further analysis will show how this affects local T_{regs} and tissue homeostasis. We observed an increase in regulatory T cell (Treg) frequencies and elevated ST2 expression in both lung and colon mucosal tissues. However, a limitation of our current study is that we did not perform comprehensive epigenetic and transcriptional profiling of the T_{regs} from these tissues, nor did we investigate the role of CREM, which has been suggested to compensate for ST2 expression from the splenic T_{regs}. These important aspects will be addressed in future studies to provide a deeper understanding of the mechanisms underlying T_{reg} function and regulation in mucosal environments. Another issue is that it is not clear how CREB activation is regulated in T_{regs}. CREB has nine serine residues in the kinase inducible domain (KID) that can be phosphorylated and activated by different kinases and different phosphorylation patterns of CREB can exert opposite effects. Further research will therefore be necessary to identify therapeutic targets to directly influence CREB activity in T_{regs}. In conclusion, we provide evidence that CREB plays a pivotal role in T_{regs}. CREB is an important transcription factor to maintain Foxp3 expression, and the interaction of CREM and CREB is crucial for the expression of ST2 in T_{regs}. A lack of CREB enhances IL-10 expression and thereby prevents Th1-mediated diseases.

Data availability statement

The datasets presented in this study can be found in online repositories. The names of the repository/repositories and accession number(s) can be found below: https://www.ncbi.nlm.nih.gov/geo/, GSE157693 https://www.ncbi.nlm.nih.gov/geo/, GSE157933.

Ethics statement

The animal study was approved by Regierungspräsident/LANUV Nordrhein-Westfalen. The study was conducted in accordance with the local legislation and institutional requirements.

Author contributions

SHS: Formal analysis, Visualization, Writing – original draft, Validation, Writing – review & editing, Methodology, Investigation. JHr: Writing – review & editing, Investigation. SS: Investigation, Writing – review & editing. TL: Writing – review & editing, Investigation. TG: Writing – review & editing, Investigation. TC: Writing – review & editing, Investigation. MS: Writing – review & editing, Investigation. MK: Writing – review & editing, Conceptualization. EV: Writing – review & editing, Investigation. SB: Investigation, Writing – review & editing. CN: Writing – review & editing, Investigation. IC: Formal analysis, Writing – review & editing. ZL: Writing – review & editing, Formal Analysis. LG: Formal analysis, Writing – review & editing. BD: Formal analysis, Writing – review & editing. AS: Writing – review & editing, Resources. SF: Writing – review & editing, Formal analysis, Investigation. JHu: Writing – review & editing, Conceptualization, Formal analysis. ES: Writing – review & editing, Resources. TB: Resources, Writing – review & editing, Conceptualization. HW: Resources, Writing – review & editing. RW: Resources, Writing –

review & editing. RB: Resources, Writing – review & editing. BL: Writing – review & editing, Resources. MZ: Writing – review & editing, Conceptualization, Formal analysis. NW: Writing – review & editing. KO: Supervision, Project administration, Methodology, Investigation, Conceptualization, Data curation, Formal analysis, Writing – review & editing, Visualization. KT: Funding acquisition, Project administration, Visualization, Data curation, Supervision, Writing – review & editing, Conceptualization, Methodology.

Funding

The author(s) declare that financial support was received for the research and/or publication of this article. DFG grant TE339/20-1 to KT. KT and KO got support from the Interdisciplinary Centre for Clinical Research within the Faculty of Medicine at the RWTH Aachen University (IZKF grant Project number – PTD 1-7). JH and TB were supported by the DFG grant SFB/TRR355/1 (Project number:490846870).

Acknowledgments

The authors acknowledge the IZKF Flow Cytometry Facility for the use of a cell sorter (DFG grant project ID 439895892) and the genomics facility for their service.

Conflict of interest

The authors declare that the research was conducted in the absence of any commercial or financial relationships that could be construed as a potential conflict of interest.

The author(s) declared that they were an editorial board member of Frontiers, at the time of submission. This had no impact on the peer review process and the final decision.

Generative AI statement

The author(s) declare that no Generative AI was used in the creation of this manuscript.

Correction note

This article has been corrected with minor changes. These changes do not impact the scientific content of the article.

Publisher's note

All claims expressed in this article are solely those of the authors and do not necessarily represent those of their affiliated organizations, or those of the publisher, the editors and the reviewers. Any product that may be evaluated in this article, or claim that may be made by its manufacturer, is not guaranteed or endorsed by the publisher.

Supplementary material

The Supplementary Material for this article can be found online at: https://www.frontiersin.org/articles/10.3389/fimmu.2025.1601008/full#supplementary-material

References

1. Wildin RS, Ramsdell F, Peake J, Faravelli F, Casanova JL, Buist N, et al. X-linked neonatal diabetes mellitus, enteropathy and endocrinopathy syndrome is the human equivalent of mouse scurfy. *Nat Genet*. (2001) 27:18–20. doi: 10.1038/83707

2. Bennett CL, Christie J, Ramsdell F, Brunkow ME, Ferguson PJ, Whitesell L, et al. The immune dysregulation, polyendocrinopathy, enteropathy, X-linked syndrome (IPEX) is caused by mutations of FOXP3. *Nat Genet*. (2001) 27:20–1. doi: 10.1038/83713

3. Zhou X, Bailey-Bucktrout SL, Jeker LT, Penaranda C, Martínez-Llordella M, Ashby M, et al. Instability of the transcription factor Foxp3 leads to the generation of pathogenic memory T cells in *vivo*. *Nat Immunol*. (2009) 10:1000–7. doi: 10.1038/ni.1774

4. Setoguchi R, Hori S, Takahashi T, Sakaguchi S. Homeostatic maintenance of natural Foxp3(+) CD25(+) CD4(+) regulatory T cells by interleukin (IL)-2 and induction of autoimmune disease by IL-2 neutralization. *J Exp Med*. (2005) 201:723–35. doi: 10.1084/jem.20041982

5. Zorn E, Nelson EA, Mohseni M, Porcheray F, Kim H, Litsa D, et al. IL-2 regulates FOXP3 expression in human CD4+CD25+ regulatory T cells through a STAT-dependent mechanism and induces the expansion of these cells in *vivo*. *Blood*. (2006) 108:1571–9. doi: 10.1182/blood-2006-02-004747

6. Liao W, Lin JX, Leonard WJ. IL-2 family cytokines: new insights into the complex roles of IL-2 as a broad regulator of T helper cell differentiation. *Curr Opin Immunol*. (2011) 23:598–604. doi: 10.1016/j.coi.2011.08.003

7. Ohl K, Tenbrock K. Regulatory T cells in systemic lupus erythematosus. *Eur J Immunol*. (2015) 45:344–55. doi: 10.1002/eji.201344280

8. Schiering C, Krausgruber T, Chomka A, Fröhlich A, Adelmann K, Wohlfert EA, et al. The alarmin IL-33 promotes regulatory T-cell function in the intestine. *Nature*. (2014) 513:564–8. doi: 10.1038/nature13577

9. Kakkar R, Lee R. The IL-33/ST2 pathway: therapeutic target and novel biomarker. *Nat Rev Drug Discov*. (2008) 7:827–40. doi: 10.1038/nrd2660

10. Griesenauer B, Paczesny S. The ST2/IL-33 axis in immune cells during inflammatory diseases. *Front Immunol*. (2017) 24:475. doi: 10.3389/fimmu.2017.00475

11. Delacher M, Imbusch CD, Weichenhan D, Breiling A, Hotz-Wagenblatt A, Träger U, et al. Genome-wide DNA-methylation landscape defines specialization of regulatory T cells in tissues. *Nat Immunol*. (2017) 18:1160–72. doi: 10.1038/ni.3799

12. Delacher M, Imbusch CD, Hotz-Wagenblatt A, Mallm JP, Bauer K, Simon M, et al. Precursors for nonlymphoid-tissue treg cells reside in secondary lymphoid organs and are programmed by the transcription factor BATF. *Immunity*. (2020) 52:295–312.e211. doi: 10.1016/j.immuni.2019.12.002

13. Okamoto A, Fujio K, Okamura T, Yamamoto K. Regulatory T-cell-associated cytokines in systemic lupus erythematosus. *J BioMed Biotechnol*. (2011) 2011:463412. doi: 10.1155/2011/463412

14. Rubtsov YP, Rasmussen JP, Chi EY, Fontenot J, Castelli L, Ye X, et al. Regulatory T cell-derived interleukin-10 limits inflammation at environmental interfaces. *Immunity*. (2008) 28:546–58. doi: 10.1016/j.immuni.2008.02.017

15. Murai M, Turovskaya O, Kim G, Madan R, Karp CL, Cheroutre H, et al. Interleukin 10 acts on regulatory T cells to maintain expression of the transcription factor Foxp3 and suppressive function in mice with colitis. *Nat Immunol*. (2009) 10:1178–84. doi: 10.1038/ni.1791

16. Unutmaz D, Pulendran B. The gut feeling of Treg cells: IL-10 is the silver lining during colitis. *Nat Immunol*. (2009) 10:1141–3. doi: 10.1038/ni1109-1141

17. Brenner S, Prösch S, Schenke-Layland K, Riese U, Gausmann U, Platzer C. cAMP-induced Interleukin-10 promoter activation depends on CCAAT/enhancer-binding protein expression and monocytic differentiation. *J Biol Chem*. (2003) 278:5597–604. doi: 10.1074/jbc.M207448200

18. Sanin DE, Prendergast CT, Mountford AP. IL-10 production in macrophages is regulated by a TLR-driven CREB-mediated mechanism that is linked to genes involved in cell metabolism. *J Immunol*. (2015) 195:1218–32. doi: 10.4049/jimmunol.1500146

19. Wang X, Ni L, Chang D, Lu H, Jiang Y, Kim BS, et al. Cyclic AMP-responsive element-binding protein (CREB) is critical in autoimmunity by promoting th17 but inhibiting treg cell differentiation. *EBioMedicine*. (2017) 25:165–74. doi: 10.1016/j.ebiom.2017.10.010

20. Okawa H, Motohashi H, Kobayashi A, Aburatani H, Kensler TW, Yamamoto M. Hepatocyte-specific deletion of the keap1 gene activates Nrf2 and confers potent resistance against acute drug toxicity. *Biochem Biophys Res Commun*. (2006) 339:79–88. doi: 10.1016/j.bbrc.2005.10.185

21. Bleich A, Mähler M, Most C, Leiter EH, Liebler-Tenorio E, Elson CO, et al. Refined histopathologic scoring system improves power to detect colitis QTL in mice. *Mamm Genome*. (2004) 15:865–71. doi: 10.1007/s00335-004-2392-2

22. Pils MC, Bleich A, Prinz I, Fasnacht N, Bollati-Fogolin M, Schippers A, et al. Commensal gut flora reduces susceptibility to experimentally induced colitis via T-cell-derived interleukin-10. *Inflammation Bowel Dis*. (2011) 17:2038–46. doi: 10.1002/ibd.21587

23. Irizarry RA, Hobbs B, Collin F, Beazer-Barclay YD, Antonellis KJ, Scherf U, et al. Exploration, normalization, and summaries of high density oligonucleotide array probe level data. *Biostatistics*. (2003) 4:249–64. doi: 10.1093/biostatistics/4.2.249

24. Wang J, Duncan D, Shi Z, Zhang B. WEB-based GEne seT anaLysis toolkit (WebGestalt): update 2013. *Nucleic Acids Res*. (2013) 41:W77–83. doi: 10.1093/nar/gkt439

25. Garg G, Muschaweckh A, Moreno H, Vasanthakumar A, Floess S, Lepennetier G, et al. Blimp1 prevents methylation of foxp3 and loss of regulatory T cell identity at sites of inflammation. *Cell Rep*. (2019) 26:1854–1868 e1855. doi: 10.1016/j.celrep.2019.01.070

26. Corces MR, Trevino AE, Hamilton EG, Greenside PG, Sinnott-Armstrong NA, Vesuna S, et al. An improved ATAC-seq protocol reduces background and enables interrogation of frozen tissues. *Nat Methods*. (2017) 14:959–62. doi: 10.1038/nmeth.4396

27. Li Z, Schulz MH, Look T, Begemann M, Zenke M, Costa IG. Identification of transcription factor binding sites using ATAC-seq. *Genome Biol*. (2019) 20:45. doi: 10.1186/s13059-019-1642-2

28. Langmead B, Salzberg SL. Fast gapped-read alignment with Bowtie 2. *Nat Methods*. (2012) 9:357–9. doi: 10.1038/nmeth.1923

29. Li H, Handsaker B, Wysoker A, Fennell T, Ruan J, Homer N, et al. The sequence alignment/map format and SAMtools. *Bioinformatics*. (2009) 25:2078–9. doi: 10.1093/bioinformatics/btp352

30. Zhang Y, Liu T, Meyer CA, Eeckhoute J, Johnson DS, Bernstein BE, et al. Model-based analysis of chIP-seq (MACS). *Genome Biol*. (2008) 9:R137. doi: 10.1186/gb-2008-9-9-r137

31. Kim HP, Leonard WJ. CREB/ATF-dependent T cell receptor-induced FoxP3 gene expression: a role for DNA methylation. *J Exp Med*. (2007) 204:1543–51. doi: 10.1084/jem.20070109

32. Ruan Q, Kameswaran V, Tone Y, Li L, Liou HC, Greene MI, et al. Development of Foxp3(+) regulatory t cells is driven by the c-Rel enhanceosome. *Immunity*. (2009) 31:932–40. doi: 10.1016/j.immuni.2009.10.006

33. Polansky JK, Schreiber L, Thelemann C, Ludwig L, Krüger M, Baumgrass R, et al. Methylation matters: binding of Ets-1 to the demethylated Foxp3 gene contributes to the stabilization of Foxp3 expression in regulatory T cells. *J Mol Med (Berl)*. (2010) 88:1029–40. doi: 10.1007/s00109-010-0642-1

34. Zheng Y, Josefowicz S, Chaudhry A, Peng XP, Forbush K, Rudensky AY. Role of conserved non-coding DNA elements in the Foxp3 gene in regulatory T-cell fate. *Nature*. (2010) 463:808–12. doi: 10.1038/nature08750

35. Thornton AM, Lu J, Korty PE, Kim YC, Martens C, Sun PD, et al. Helios(+) and Helios(-) Treg subpopulations are phenotypically and functionally distinct and express dissimilar TCR repertoires. *Eur J Immunol*. (2019) 49:398–412. doi: 10.1002/eji.201847935

36. Drake LY, Kita H. IL-33: biological properties, functions, and roles in airway disease. *Immunol Rev*. (2017) 278:173–84. doi: 10.1111/imr.12552

37. Siede J, Fröhlich A, Datsi A, Hegazy AN, Varga DV, Holecska V, et al. IL-33 receptor-expressing regulatory T cells are highly activated, th2 biased and suppress CD4 T cell proliferation through IL-10 and TGFbeta release. *PloS One*. (2016) 11:e0161507. doi: 10.1371/journal.pone.0161507

38. Holgado A, Braun H, Van Nuffel E, Detry S, Schuijs MJ, Deswarte K, et al. IL-33trap is a novel IL-33-neutralizing biologic that inhibits allergic airway inflammation. *J Allergy Clin Immunol*. (2019) 144:204–15. doi: 10.1016/j.jaci.2019.02.028

39. Suliman HB, Sweeney TE, Withers CM, Piantadosi CA. Co-regulation of nuclear respiratory factor-1 by NFkappaB and CREB links LPS-induced inflammation to mitochondrial biogenesis. *J Cell Sci*. (2010) 123:2565–75. doi: 10.1242/jcs.064089

40. Miragaia RJ, Gomes T, Chomka A, Jardine L, Riedel A, Hegazy AN, et al. Single-cell transcriptomics of regulatory T cells reveals trajectories of tissue adaptation. *Immunity*. (2019) 50:493–504 e497. doi: 10.1016/j.immuni.2019.01.001

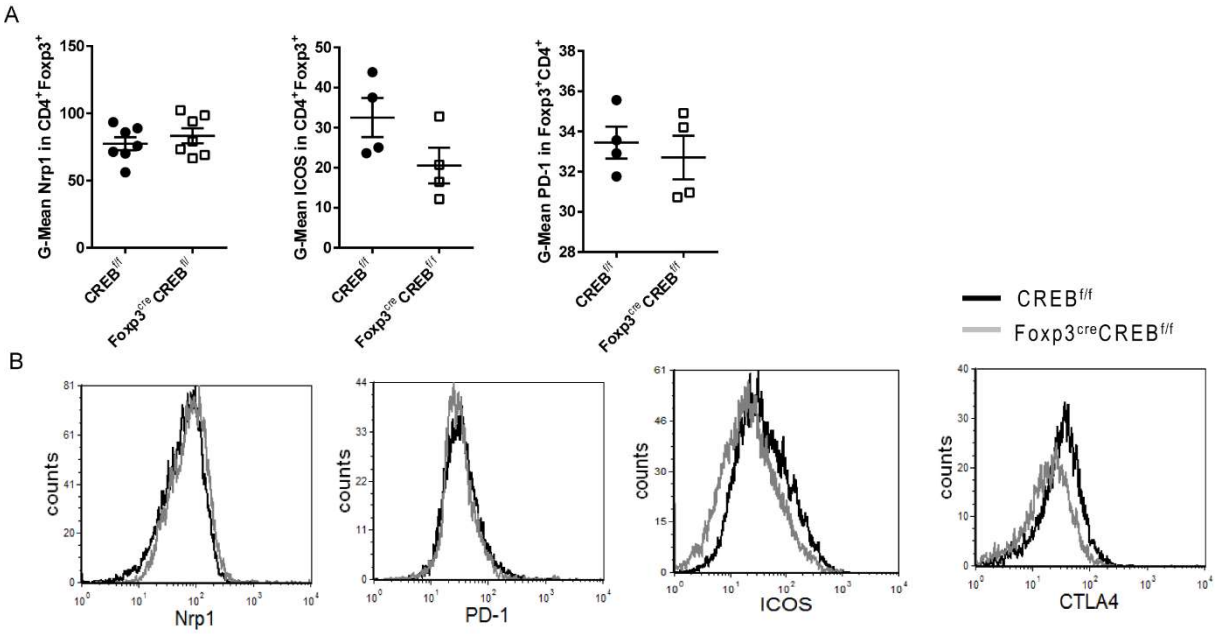
41. Kuhn R, Löhler J, Rennick D, Rajewsky K, Müller W. Interleukin-10-deficient mice develop chronic enterocolitis. *Cell*. (1993) 75:263–74. doi: 10.1016/0092-8674(93)80068-P

42. Spencer SD, Di Marco F, Hooley J, Pitts-Meek S, Bauer M, Ryan AM, et al. The orphan receptor CRF2–4 is an essential subunit of the interleukin 10 receptor. *J Exp Med*. (1998) 187:571–8. doi: 10.1084/jem.187.4.571

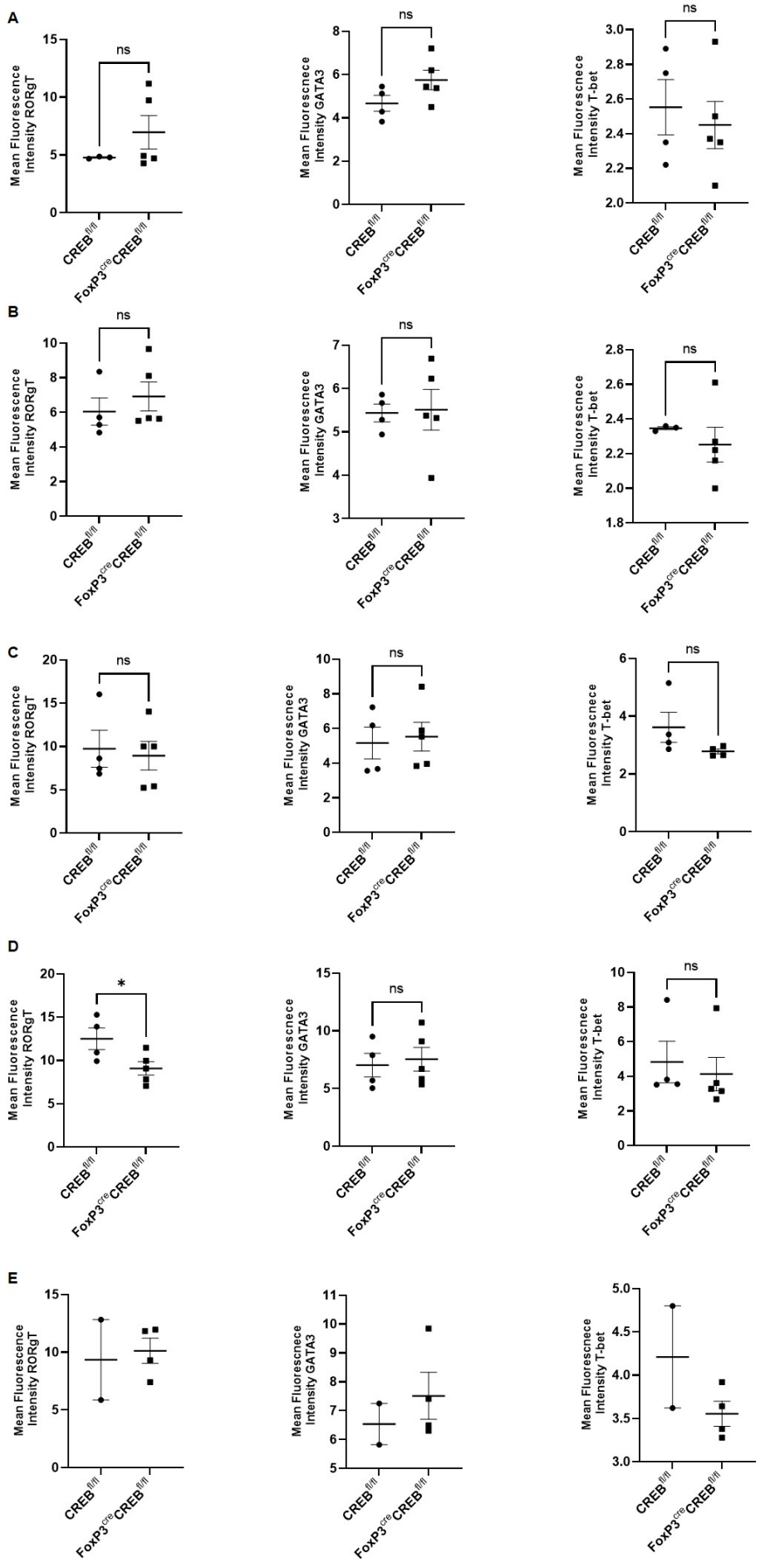
43. Spath S, Roan F, Presnell SR, Höllbacher B, Ziegler SF. Profiling of Tregs across tissues reveals plasticity in ST2 expression and hierarchies in tissue-specific phenotypes. *iScience*. (2022) 25:104998. doi: 10.1016/j.isci.2022.104998

APPENDIX B

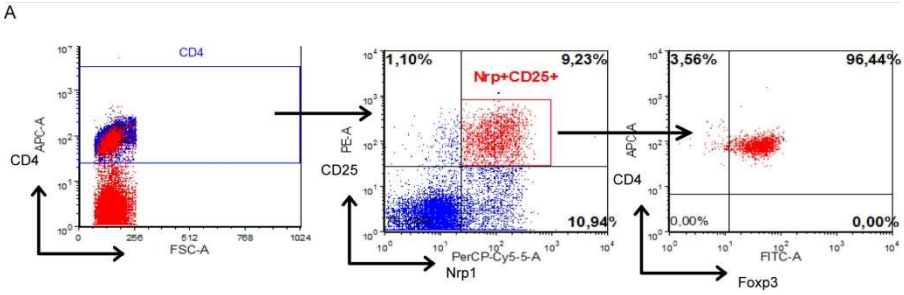
SUPPLEMENTARY FIGURES



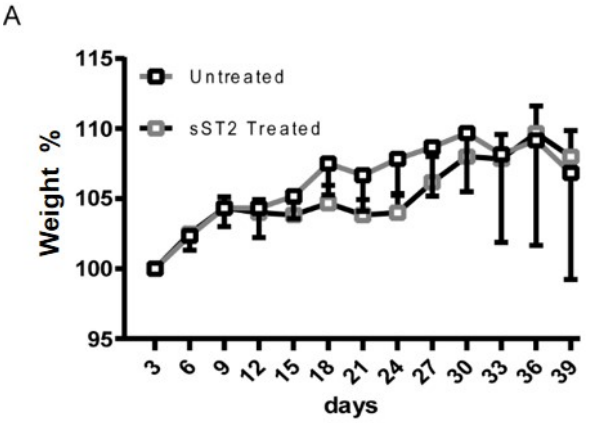
Supplementary Figure 1: Characterization of CREB-deficient T_{reg} cells. A) Statistical analysis and **B)** representative histograms of T_{reg} cell markers in $CD4^{+}Foxp3^{+}$ splenic cells. Mice were 6-9 weeks old, and sex and age matched. For A, results are expressed as the mean ± SEM.


A
B
C
D
E
Mean Fluorescence Intensity RORgT
Mean Fluorescnece Intensity GATA3
Mean Fluorescnece Intensity T-bet
ns
*
CREB fl/fl
FoxP3cre CREB fl/fl

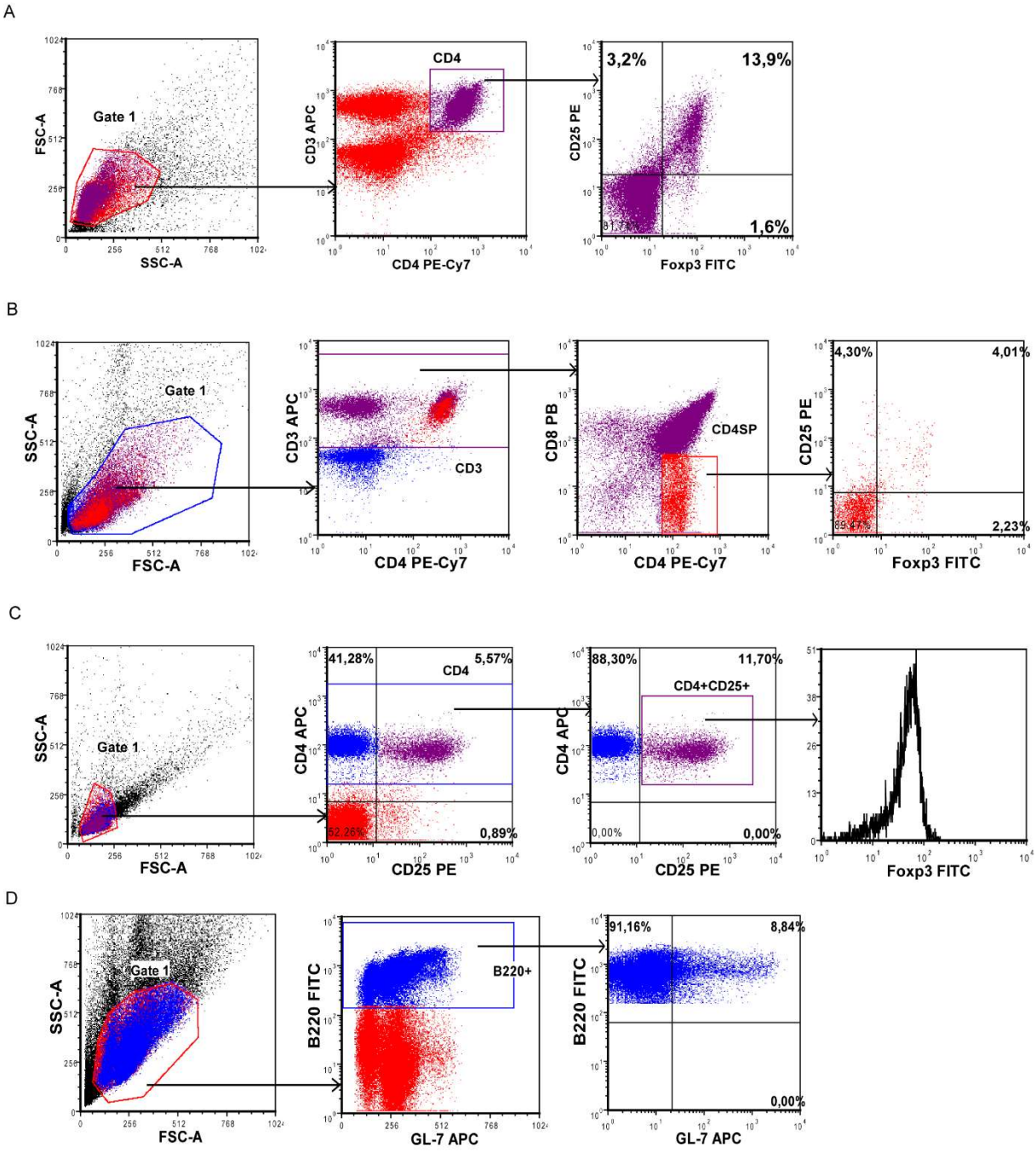
Supplementary Figure 2: Expression of T_h-lineage transcription factors in different organs. Mean-fluorescent intensity of RORγt, GATA3 and T-bet expression in $CD45^+CD4^+Foxp3^+$ cells in **A)** Spleen, **B)** Mesenteric lymph node, **C)** Lung, **D)** Liver, and **E)** Colon. Each dot represents one animal. ns - $p>0.05$, *$p<0.05$ and results are expressed as the mean ± SEM.



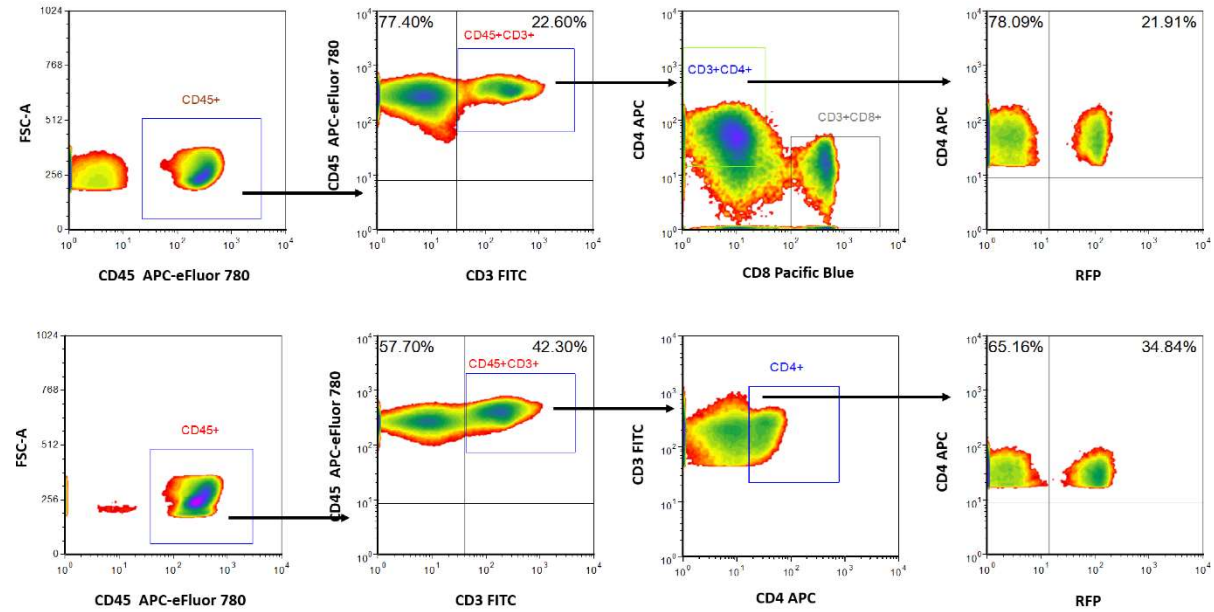
Supplementary Figure 3: Gating strategy to sort T_{reg} cells. We sorted $Nrp1^{+}CD25^{+}CD4^{+}$ cells and thereby achieved a purity of 96% $Foxp3^{+}$ cells.



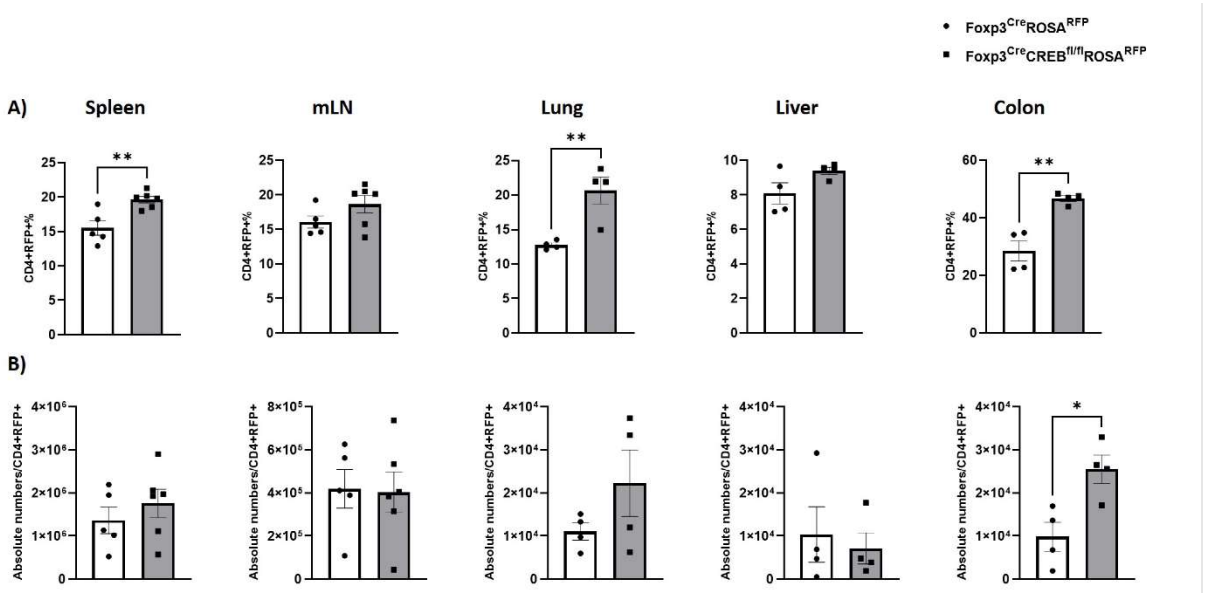
Supplementary Figure 4: Reduced colitis in *Foxp3^{cre}CREB$^{fl/fl}$* CD4^{+} T cell recipients is unaffected by ST2 blockade. A) Rag2$^{-/-}$ mice were adoptively transferred with *Foxp3^{cre}CREB$^{fl/fl}$* CD4^{+} T cells (CD4+CD25-). Mice were either treated with sST2 or PBS. Body weight is shown as percentage of starting weight (*N = 6*, symbols indicate mean and error bars represent means ±SEM).



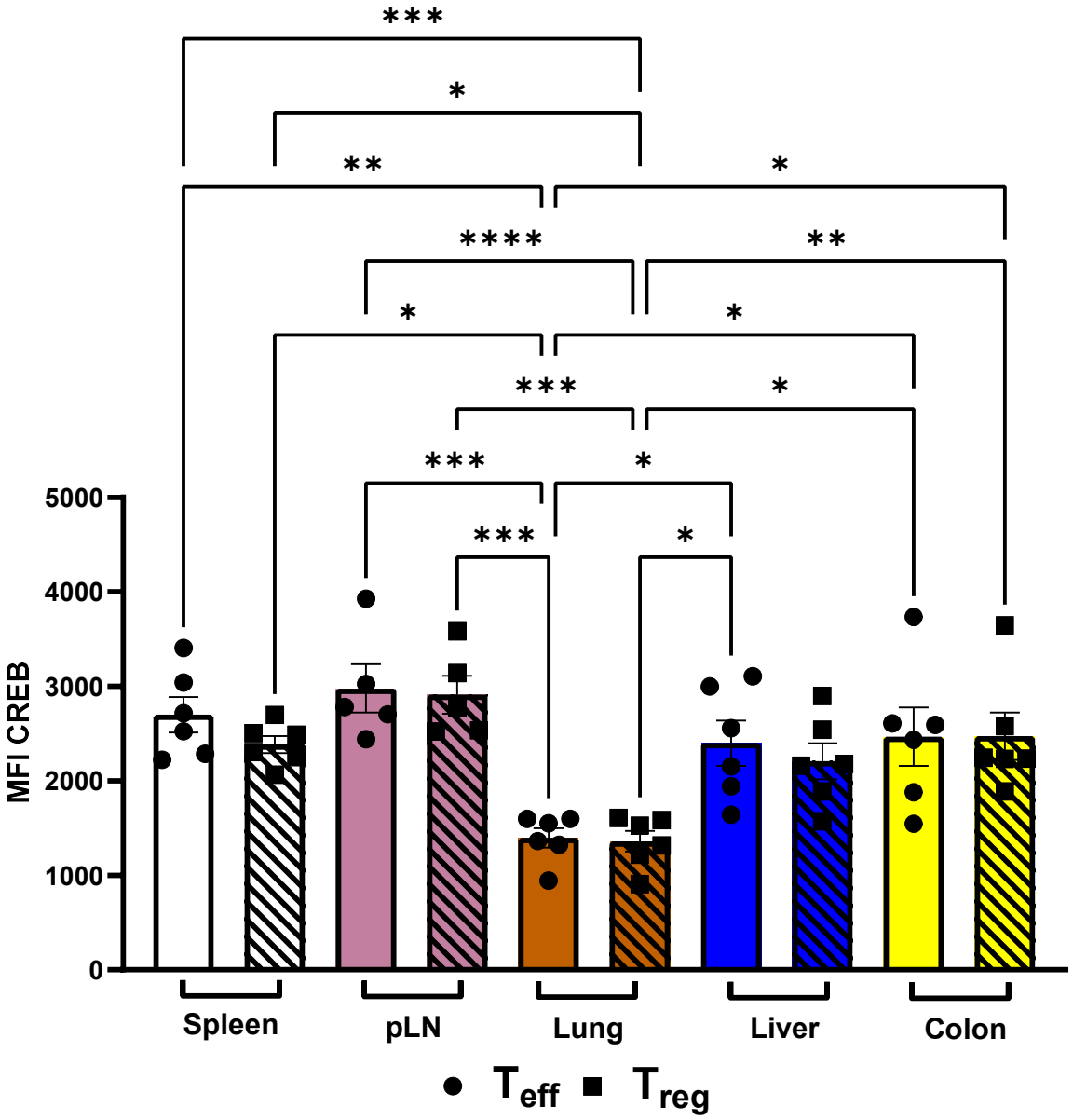
Supplementary Figure 5: Gating strategies. A) Figure exemplifying gating strategy to determine $CD25^+Foxp3^+$ T_{regs} within LNs and spleens. **B)** Figure exemplifying gating strategy to determine $CD25^+Foxp3^+$ T_{regs} within thymus. **C)** Figure exemplifying gating strategy to determine Foxp3 MFI within $CD4^+CD25^+$ cells. **D)** Figure exemplifying gating strategy to determine percentages of $GL\text{-}7^+$ cells within $B220^+$ cells.



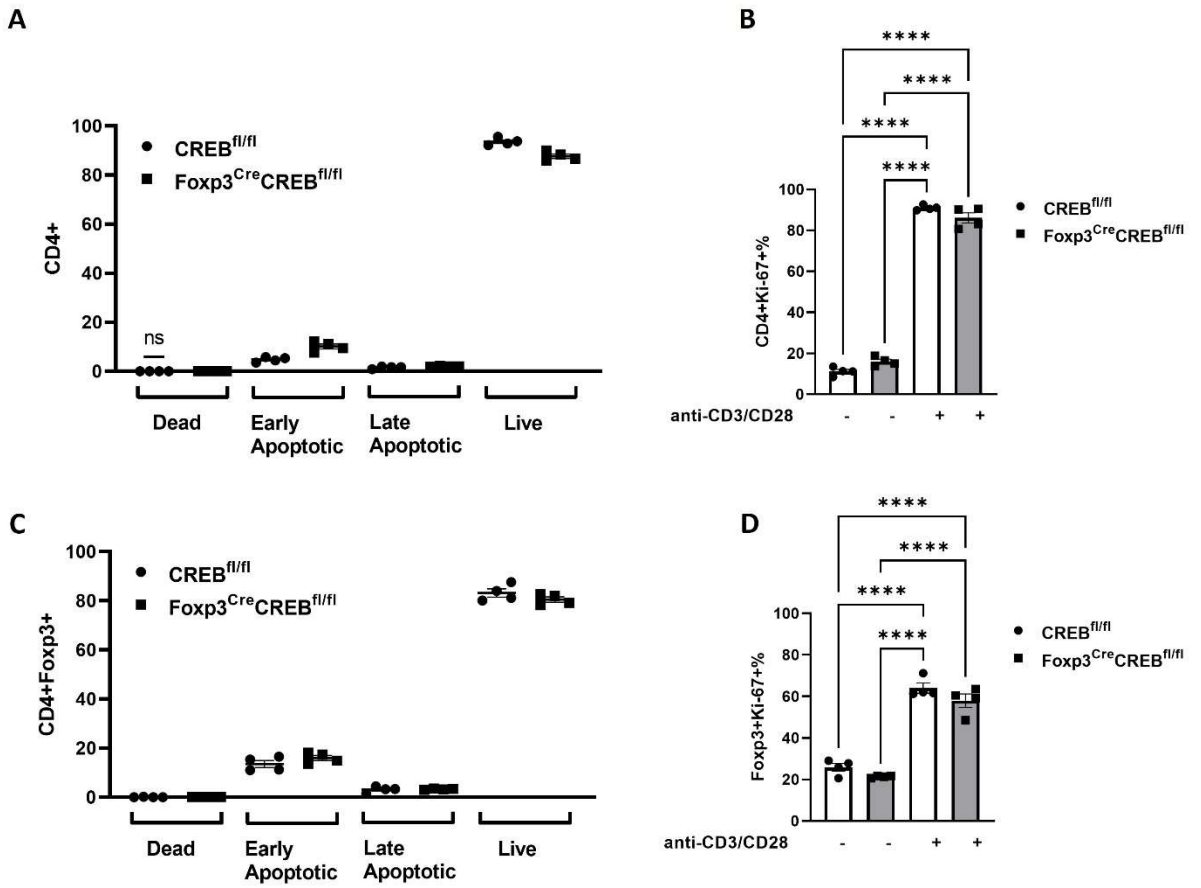
Supplementary Figure 6: Gating strategies used in *Foxp3^{cre}ROSA^{RFP}* mice. Figure exemplifying gating strategy to determine T_{regs} within **A)** lung and **B)** colon.



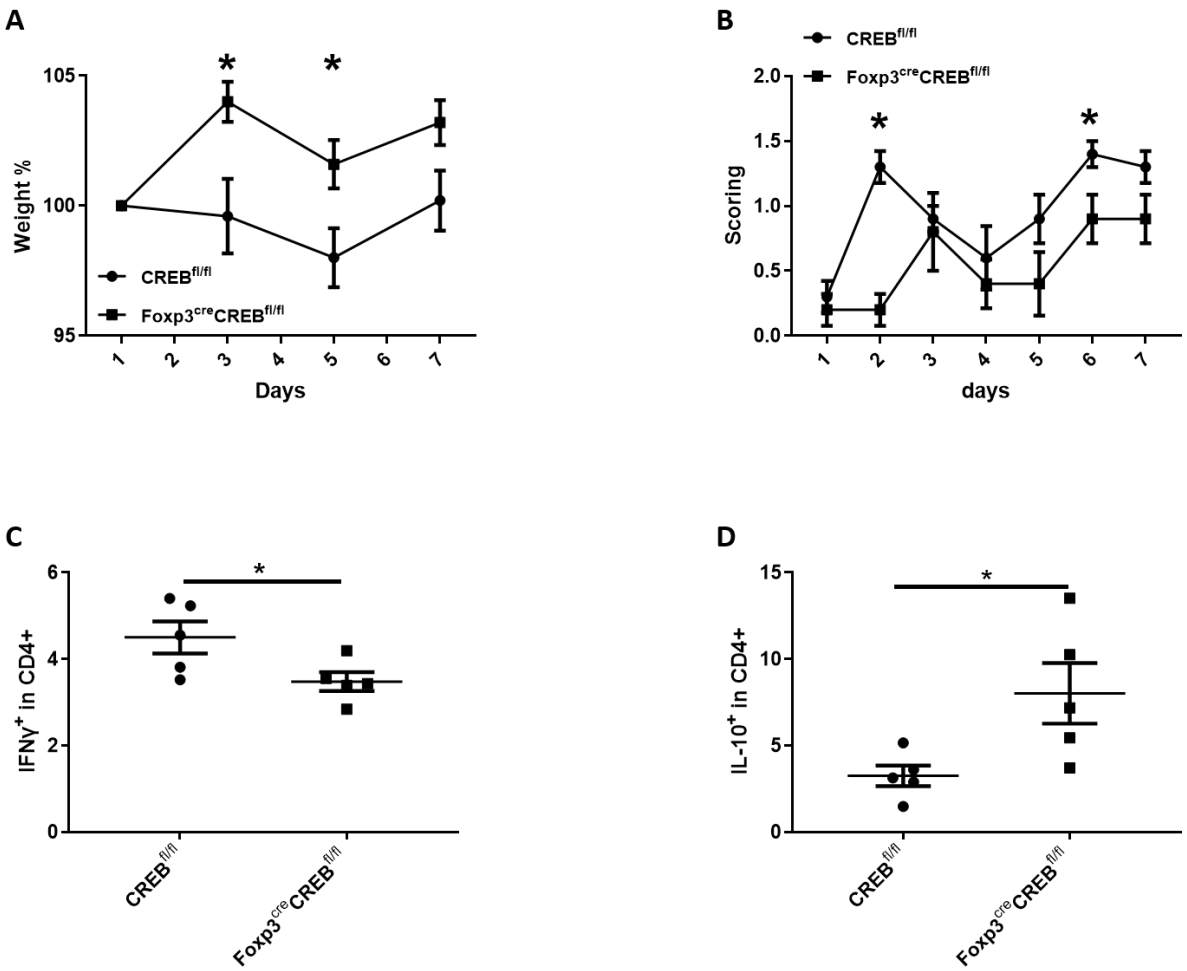
Supplementary Figure 7: Cell frequencies **A)** and absolute cell numbers **B)** of RFP+ cells in spleens, mLN (mesenteric lymph nodes), lungs, livers and colons of Foxp*3*^{cre}*ROSA*^{RFP} and *Foxp3*^{cre}*CREB*$^{fl/fl}$*ROSA*^{RFP} mice. Unpaired Student t-test was performed. **p<0.01 and results are expressed as the mean ± SEM.



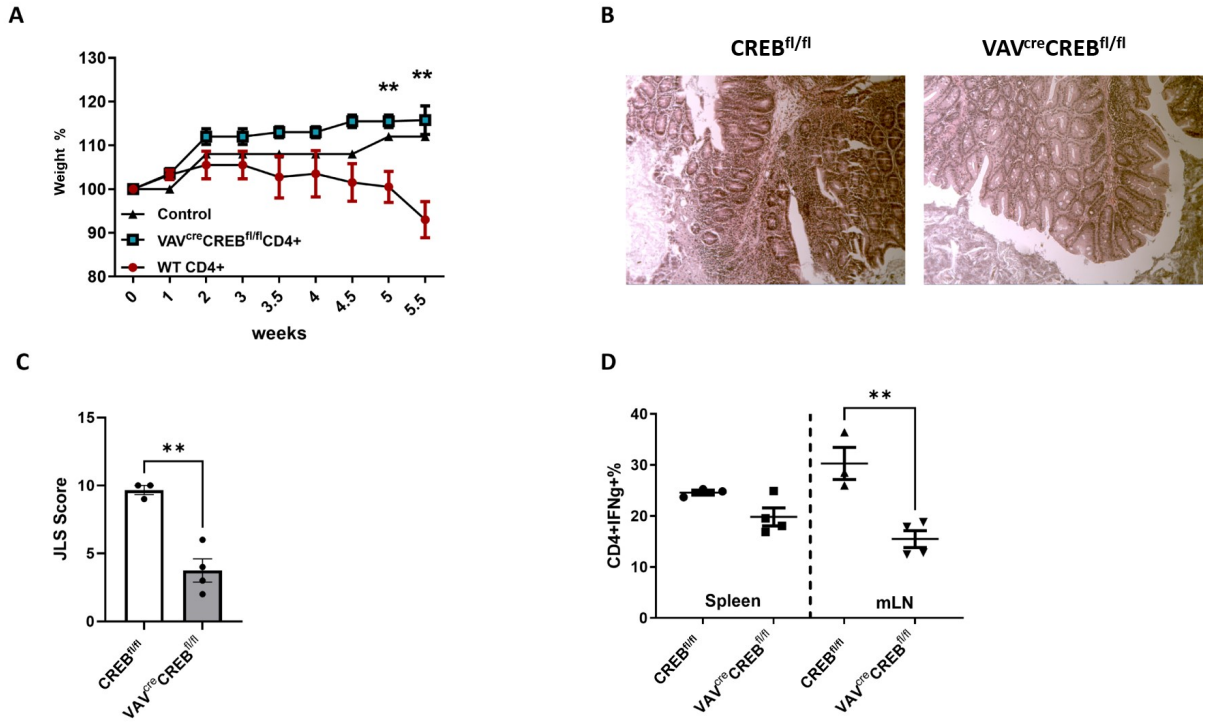
Supplementary Figure 8: Expression of CREB on T_{eff} and T_{reg} cell populations in Spleens, peripheral Lymph nodes, Lungs, Livers and colons of Foxp3^{cre}*ROSA*^{RFP} mice. ONE-way ANOVA test was performed. *p<0.05, **p<0.01, ***p<0.001, ****p<0.0001 and results are expressed as the mean ± SEM.



Supplementary Figure 9: Splenocytes of *WT and Foxp3^{cre}CREB$^{fl/fl}$* mice were stimulated with anti-CD3/CD28 for 2 days and stained for cell survival and proliferation. Annexin and Fixable viability-stained cells of **A)** CD4+ & **C)** CD4+Foxp3+ cells. Ki-67-stained cell percentages of **B)** CD4+ & **D)** CD4+Foxp3+ cells. ONE way-ANOVA test was performed. ns – $p>0.05$, ****$p<0.0001$ and results are expressed as the mean ± SEM.



Supplementary Figure 10: *Foxp3^{cre}CREB$^{fl/fl}$* mice only develop moderate signs of inflammation in an EAE model. EAE was induced in female mice (*N = 5* CREB$^{fl/fl}$ and *N = 5 Foxp3^{cre}CREB$^{fl/fl}$* mice). A) Loss of weight and B) EAE score were measured beginning after onset of symptoms. C) Statistical analysis of IFN-γ^+ cells within splenic CD4$^+$ T cells. D) Statistical analysis of IL-10$^+$ cells within splenic CD4$^+$ T cells, two tailed unpaired t-test, each dot represents one animal, error bars SEM, *N = 5* CREB$^{fl/fl}$ and *N = 5 Foxp3^{cre}CREB$^{fl/fl}$*.



Supplementary Figure 11: *Vav^{cre}Creb$^{fl/fl}$* CD4+ T cells induce only moderate inflammation in experimental colitis. Rag$^{-/-}$ mice were adoptively transferred with CD4^{+} wild-type cells (*CREB$^{fl/fl}$* CD4^{+}) or *Vav^{CRE}CREB$^{fl/fl}$* CD4^{+} T cells. Untreated Rag$^{-/-}$ mice were used as controls (K). Mice were weighed and sacrificed 5 weeks after transfer. (A) Body weight as a percent of starting weight. (B) Representative photomicrographs of hematoxylin and eosin (H&E)-stained colon sections imaged using a 10x objective. C) Results of histological TJL (The Jackson Laboratory Score) scoring of colon sections (one independently performed experiments, *CREB$^{fl/fl}$* recipients N = 3, *VAV^{cre}CREB$^{fl/fl}$* recipients N = 4). D) Statistical analysis of IFNy within CD4^{+} cells in spleen and mLNs (*CREB$^{fl/fl}$* recipients N = 3, *VAV3^{cre}CREB$^{fl/fl}$* recipients N = 4), a two-tailed, unpaired t-test was used.

scientific reports

Check for updates

OPEN

Tofacitinib fails to prevent T cell transfer colitis in mice but ameliorates disease activity

Sudheendra Hebbar Subramanyam, Judit Turyne Hriczko, Angeliki Pappas, Angela Schippers, Nobert Wagner, Kim Ohl & Klaus Tenbrock✉

Tofacitinib is a JAK inhibitor approved for ulcerative colitis in humans. Despite of its' proven effectiveness in humans, mechanistic data are scarce on the effectiveness of Tofactinib in experimental colitis in mice. We induced experimental colitis by transfer of CD4+CD25− isolated T cells into RAG2−/− (T and B cell deficient) mice and treated these mice with tofacitinib for 5–6 weeks either with a dosage of 10 or 40 mg/kg body weight immediately after CD4+ transfer or started treatment after first symptoms of disease for several weeks. While treatment with tofacitinib immediately after transfer resulted in an enhanced expansion of CD4+ T cells and did not prevent occurrence of colitis, treatment after start of symptoms of colitis ameliorated disease activity on a clinical basis and in histological analyses. Tofacitinib is effective in the treatment of murine experimental T cell transfer colitis, however does not prevent occurrence of disease.

The incidence of inflammatory bowel diseases (IBD) is rising and imposes a tremendous disease burden on the individual patient and also on society due to the often life-long need for immune suppression, involving high costs (biologicals) or severe side-effects (corticosteroids) and numerous days of sick leave. The exact etiology of the diseases is unknown, but involves multiple pathogenic factors including environmental changes, genetic predisposition, an abnormal gut microbiota and a broadly dysregulated immune system[1,2]. The therapy of ulcerative colitis (UC) is challenging. In spite of increasing therapeutic options, UC remains a disease with a high individual morbidity and relevant treatment costs. Moreover, reliable disease parameters for the guidance of treatment are lacking. Especially cytokines drive intestinal inflammation and pathologic processes associated with IBD. Janus kinases (JAKs) are central mediators of intracellular cytokine signaling and their blockade can interfere with more than 50 cytokines[3–5]. They are activated by extracellular cytokine receptors, which induces JAK-mediated receptor phosphorylation and facilitates activation of Signal Transducer and Activator of Transcription proteins (STATs), which then translocate to the nucleus and induce gene transcription[4,5]. It is therefore not surprising that dysregulations in JAK/STAT signaling are implicated in several inflammatory and autoimmune diseases[7]. The pan-JAK inhibitors including tofacitinib have been proven efficient in the treatment of UC and are approved for the treatment as second line option after failure of conventional disease modifying drugs. Despite this approval and despite the wealth of in vitro data on tofacitinib, surprisingly in vivo data on the effectiveness on colitis in mice are scarce. All published models are primarily models of chemically induced colitis (either DSS or oxazolone)[6–10]. One very recently publication included a humanized model[11]. To investigate the clinical effect of tofacitinib in mice, we performed a CD4+ transfer colitis into lymphopenic Rag2−/− mice and treated the mice with tofacitinib dissolved in the drinking water. Treatment with tofacitinib immediately after CD4+ transfer resulted in an enhanced expansion of inflammatory CD4+ T cells and did not prevent occurrence of colitis, however, treatment after start of symptoms of colitis ameliorated disease activity on a clinical basis and histological analyses.

Results

Low dose tofacitinib treatment does not prevent onset of colitis

To induce transfer colitis, RAG2−/− mice were adoptively transferred with 2×10^6 $CD4^+$ $CD25^-$ T cells. Initially, mice received 0.05 mg/ml tofacitinib in the drinking water, which results in a dosage of about 10 mg/kg/day bodyweight per day (low dose treatment). The control group received normal drinking water. As shown in Fig. 1A, onset and progression of weight loss did not differ between the group treated with tofacitinib and the untreated mice. In addition, colon histologies did not show any difference in the mice with and without treatment

Department of Pediatrics, RWTH Aachen University, Pauwelsstr 30, 52074 Aachen, Germany. ✉email: ktenbrock@ukaachen.de

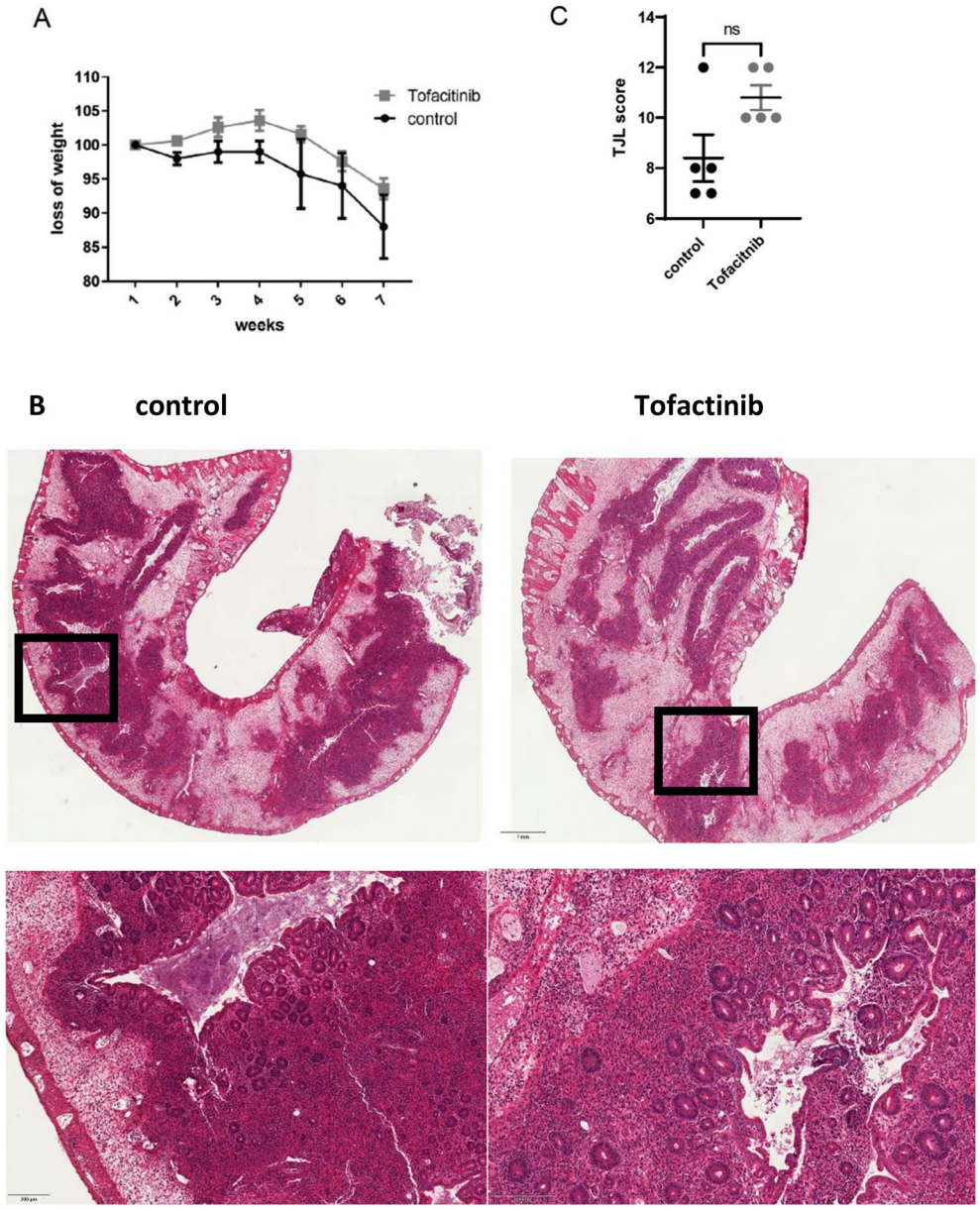


Figure 1. Low-doses of tofacitinib has no effect on disease activity in experimental colitis. Rag−/− mice were adoptively transferred with $CD4^+CD25$-wild-type cells. Mice were weighed weekly and sacrificed 7 weeks after transfer. (**A**) Loss of body weight, two-tailed unpaired t-test were used to test for significance (one experiment with N = 4 controls, N = 5 Tofacitinib treated mice). (**B**) Representative histology of colon tissue (left: control, right: tofactinib), (**C**) Results of histological TJL (The Jackson Laboratory Score) scoring of colon sections.

(Fig. 1B,C). Mice were sacrificed after 7 weeks, and flow cytometric and histological analyses were performed. Cell populations in the spleen and the mesenteric lymph nodes (mLNs) differed between treated and untreated mice. We found enhanced splenic numbers of CD3+ CD4+ cells as well as CD11b+ Gr1+ myeloid derived suppressor cells, while numbers in mLNs were not different except from decreased expression of Foxp3+ Tregs in tofacitinib treated animals (Fig. 2A,B). Regarding percentages of CD4+ cells, only Foxp3+ cells in the spleen were reduced, the rest showed no statistical differences (Fig. 2C–H). Regarding cytokine expression, percentages of interleukin 17 (IL-17) producing CD4+ T cells in spleens and mLNs of tofacitinib treated mice were enhanced, while percentages of IFN-γ producing CD4+ T cells was reduced (Fig. 2I–L). Summing up, low dose tofacitinib starting immediately after transfer during the expansion phase of CD4+ T cells enhances splenic numbers of CD3+ CD4+ T cells as well as of MDSCs and does not prevent colonic inflammation.

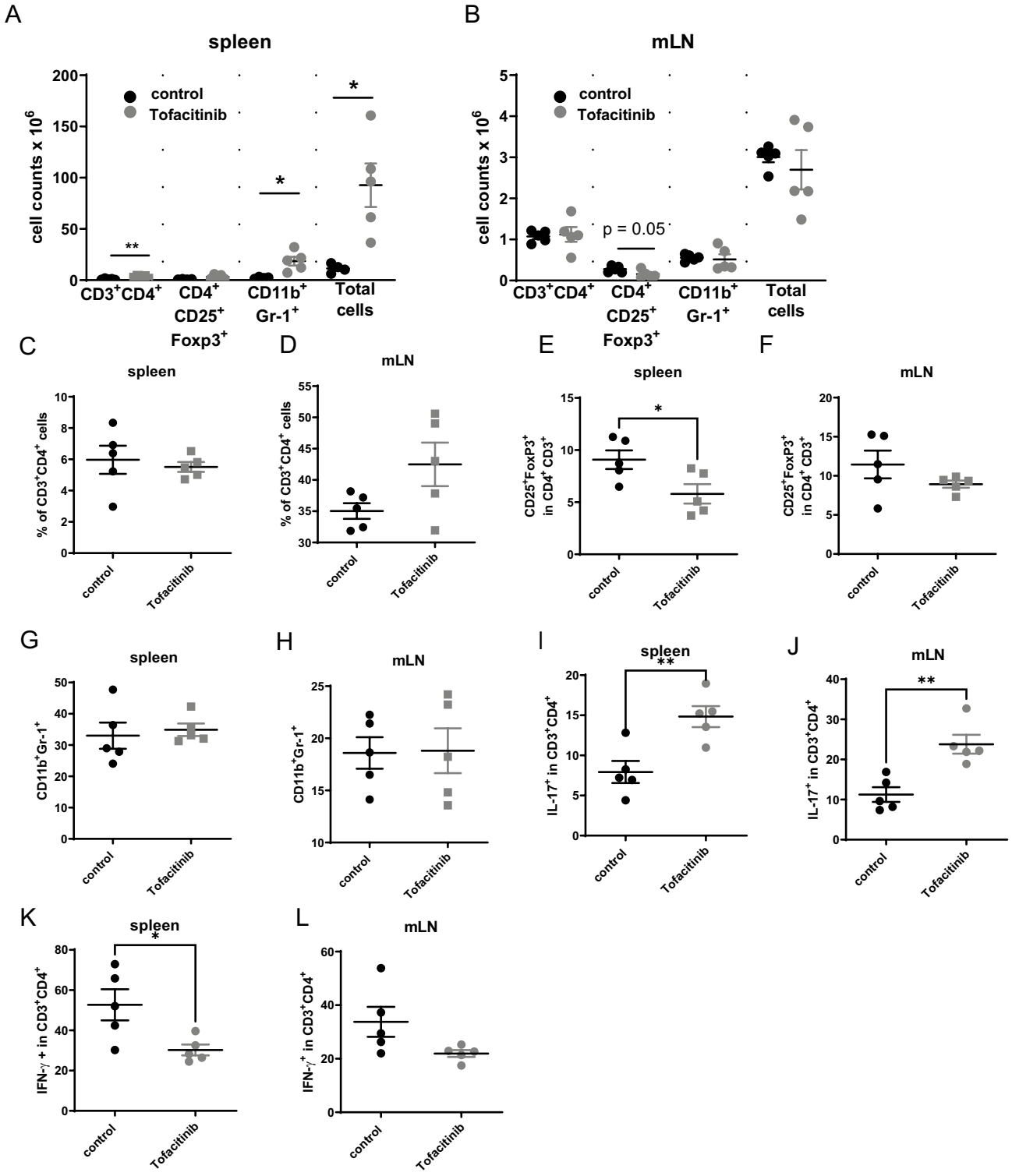


Figure 2. Low-doses of tofacitinib does not influence immune cell activation. (**A**) Absolute numbers of immune cells within the spleens assessed by flow cytometry (N = 4 controls, N = 5 Tofacitinib treated mice, two-tailed unpaired t-test were used). (**B**) Absolute numbers of immune cells within the mLNs assessed by flow cytometry (N = 5 controls, N = 5 Tofacitinib treated mice, p = 0.0084). Flow cytometric analysis was performed to determine percentages of (**C**) CD3+ CD4+ T cells within the spleen (** = 0.0084, * = 0.0121, * = 0.0120). (**D**) CD3+ CD4+ T cells within mLN. (**E**) % of CD25+ Foxp3+ in CD4+ CD3+ cells in the spleen (* = 0.034). (**F**) CD4+ CD3+ CD25+ Foxp3+ cells in the mLNs. (**G**) CD11b + Gr-1 + cells in the spleen. (**H**) CD11b + Gr-1 + cells within mLN. (**I**) IL17+ T cells within the spleen (** = 0.0066). (**J**) IL-17+ T cells within mLN (** = 0.0030). (**K**) IFN-γ+ T cells within the spleen (* = 0.0253). (**L**) IFN-γ+ T cells in mLN. In all data sets each dot represents one animal, error bars SEM, two-tailed unpaired t-tests were used to test for significance.

High dose tofacitinib treatment does not prevent onset of colitis

After these rather unexpected results, we used a higher dosing regimen of tofacitinib. After adoptive transfer, mice received 0.2 mg/ml tofacitinib in the drinking water, which results in a dosage of about 40 mg/kg/day bodyweight per day (high dose treatment). Again, and comparable to the data in the low dose treated mice, tofacitinib treated mice developed disease and weight loss similar to control mice (Fig. 3A). Colon histology showed no statistical differences (Fig. 3B). The same was true for numbers and percentages of T cells including IFN-γ and IL-17 producing cells in spleen and mLN (Fig. 4A–G). Only expression of MDSCs was slightly different in terms of percentages of CD11b+ Gr-1+ cells showing more MDSCs in spleens of tofacitinib treated mice and less in the mLNs compared to untreated mice (Fig. 4H–J). We furthermore isolated RNA of whole colon and preformed real time PCR using primers for IL1β, IL-17, IFN-γ and TNFα. Colonic samples of tofacitinib treated mice showed higher expression of IL-17, IFN-γ and TNFα (Fig. 5A).

High dose tofacitinib treatment ameliorates disease after onset of colitis

We next decided to adopt a "treatment" regime, which started after onset of first symptoms defined by loss of weight in the first mouse. This was around 2 weeks after adoptive transfer. We again supplied the mice with 0.2 mg/ml tofacitinib in the drinking water, which represented a dosage of about 40 mg/kg/day bodyweight. This treatment protocol resulted in a stabilization of the bodyweight in tofacitinib treated mice (Fig. 6A) and in an amelioration of disease with lower inflammation in the histologic colon samples (Fig. 6B,C). Moreover, percentages of IFN-γ producing T cells in spleens and mLNs were reduced in the tofacitinib treated mice (Fig. 7A,B), while there was no difference in the percentages of IL-17 producing T cells (Fig. 7C,D). Numbers of CD11b+ Gr1+ myeloid derived suppressor cells were comparable in both groups (not shown) as well as cytokine mRNA expression (Fig. 7E).

Discussion

Our data demonstrate that treatment with tofacitinib has different effects on the clinical outcome of T cell transfer colitis depending on the onset of treatment. Treatment that starts immediately after T cell transfer does not prevent disease. If anything, it even results in aggravation of disease represented by colonic histology and expression of inflammatory cytokines in T cells and in colonic RNA. If treatment is started after the onset of first symptoms, tofacitinib ameliorated disease shown by weight stabilization, colonic histology and decreased production of inflammatory cytokines.

Our findings of the therapeutic effect of tofacitinib were somehow expected and go in line with a recent paper from Lechner et al., which described effectiveness in the treatment of oxazolone induced colitis with downregulation of T cell derived cytokines like IL-5, IL-6, IL-9, IL-13 and IL-17A[7]. This colitis model is mediated by a hypersensitivity reaction related to oxazolone after sensitization and therefore primarily CD8 mediated. In addition, tofacitinib exerts a similar effect on human organoids from UC and control endoscopies, where tofacitinib reduces inflammatory cytokines by inhibition of pSTAT1/3 expression in T-cells[12]. In vitro experiments indicated that the effects of tofacitinib were mediated through suppression of IL-17 and IFN-γ production and proliferation of CD4 T cells, presumably Th1 and Th17. In an autoimmune lymphoproliferative (ALPS) mouse model, tofactinib treatment decreased expression of TCRαβ(+)CD4(-)CD8(-)T lymphocyte numbers while it increased CD8(+) T cells without a remarkable effect on CD4(+) lymphocytes including FoxP3(+) regulatory T cells[13].

We were surprised to find no effect on colonic inflammation and even an expansion of CD4+ T cell numbers in the mice that were treated directly after adoptive transfer of T cells. This is in contrast to CD4+ T-cell-mediated murine acute graft-versus-host disease, which can be prevented by tofacitinib. This is related to inhibition of the interferon-γ pathway[14]. It has been shown before that human T-lymphocyte proliferation is inhibited by

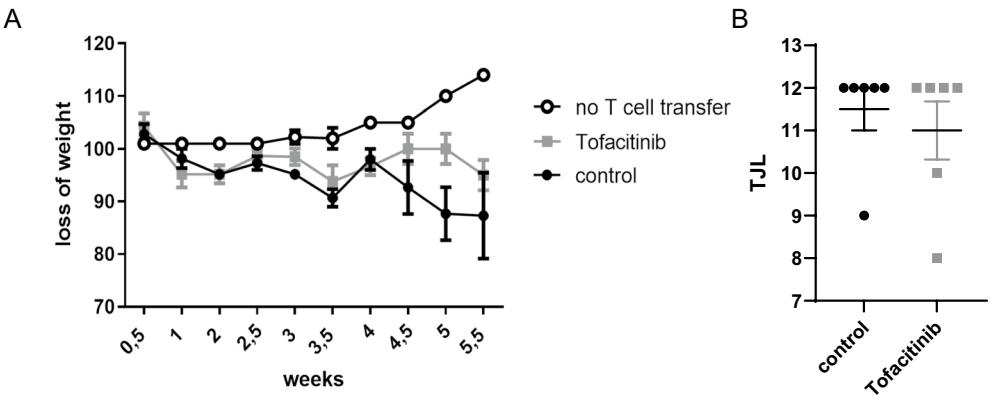


Figure 3. High-dose Tofacitinib treatment does not prevent weight loss and intestinal inflammation. Rag−/− mice were adoptively transferred with $CD4^+$ CD25- wild-type cells Untreated Rag−/− mice were used as controls (**A**) Weight loss (N = 6 control mice, 6 Tofacitinib-treated mice and 4 mice without T cell transfer, one experiment). (**B**) Results of histological TJL (The Jackson Laboratory Score) scoring of colon sections.

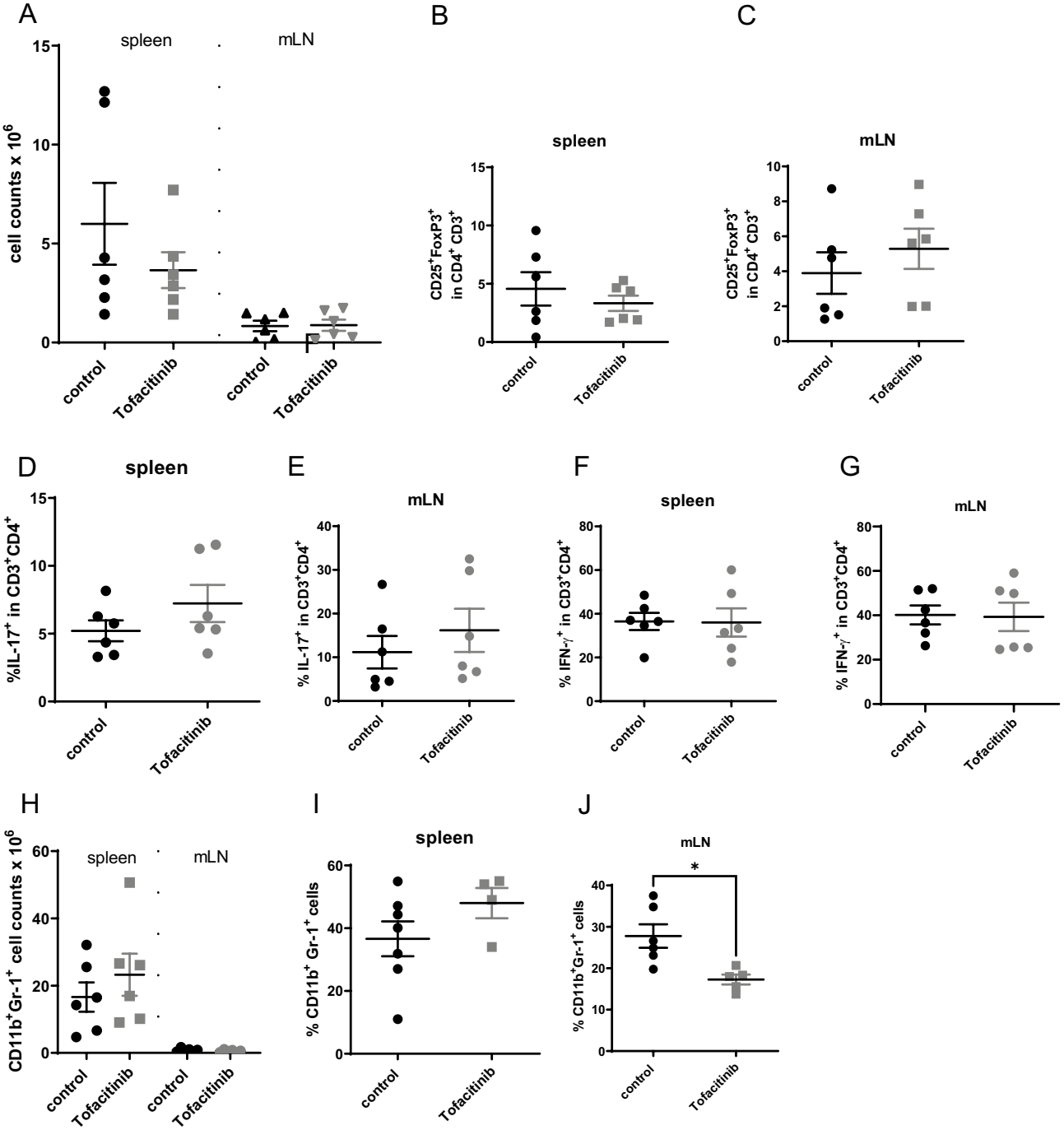


Figure 4. High-dose Tofacitinib treatment does not increase immune cell numbers. (**A**) Absolute numbers of immune cells within the spleens and mLNs assessed by flow cytometry. (**B**) Statistical analysis of CD4+ CD3+ CD25+ Foxp3+ cells in the spleen, N = 6 mice in each group). (**C**) Statistical analysis of CD4+ CD3+ CD25+ Foxp3+ cells in the mLNs, N = 6 mice in each group). (**D**) Statistical analysis of IL-17+ T cells within the spleen, N = 6 mice in each group). (**E**) Statistical analysis of IL-17+ T cells within mLNs, N = 6 mice in each group). (**F**) Statistical analysis of IFN-γ+ T cells within the spleen, N = 6 mice in each group). (**G**) Statistical analysis of IFN-γ+ T cells within mLNs, N = 6 mice in each group). (**H**) Absolute numbers of CD11b + Gr-1 + cells within the spleen and mLNs assessed by flow cytometry, N = 6 mice in each group. (**I**) Statistical analysis of CD11b + Gr-1 + cells within spleen, N = 6 control mice and N = 4 Tofactinib treated mice. (**J**) Statistical analysis of CD11b + Gr-1 + cells within spleen, N = 6 control mice and N = 5 Tofacitinib treated mice (* = 0.0112). For all data sets error bars indicate SEM, two-tailed unpaired t-tests were used to test for significance.

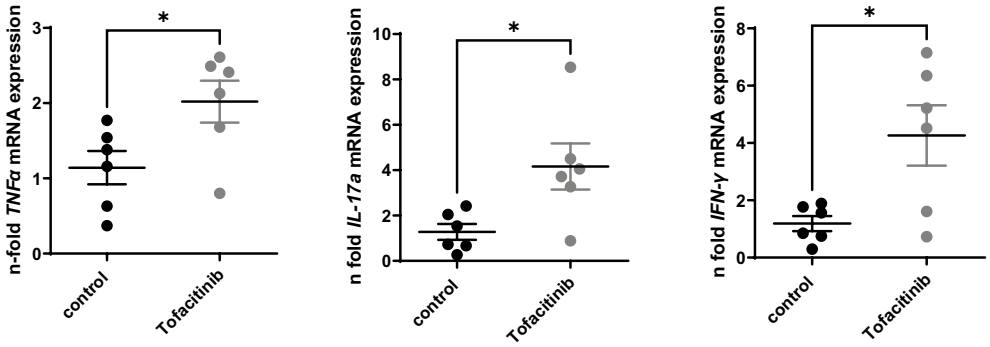


Figure 5. Inflammatory cytokines in the colon are enhanced by high dose Tofacitinib treatment. Expression of inflammatory cytokines analyzed by RT-qPCR, N = 6 mice in each group, two-tailed unpaired t-tests were used to test for significance (* = 0.0333, * = 0.0230, * = 0.0176).

tofacitinib, however antiproliferative effects are strongly attenuated, when tofacitinib is given to preactivated PBMCs, which suggests that the surrounding conditions play a pivotal role[15]. Moreover, and again in humans, during phase III studies in patients with rheumatoid arthritis with more than 7000 patients, tofacitinib treatment resulted in an initial increase in lymphocyte counts within the first 3 months versus pretreatment baseline, which gradually declined to steady state by ~ 48 months[16]. In addition, it was shown before that low dose tofacitinib accelerates the onset of experimental autoimmune encephalomyelitis by potentiating Th17 differentiation[17]. This goes in line with our first experiment, in which we also found an enhancement of IL-17 producing cells. Thus, apart from timing also dosage might play a critical role. However, other publications suggest that tofacitinib inhibits proliferation in CD4+ and CD8 + T cells as well as Th1 and Th17 differentiation in vitro, while Th2 and regulatory T cell lineages remained unaffected[6]. Moreover tofacitinib is efficacious in patients with active UC but not Crohn's disease (CD), which can be explained that JAK/STAT molecules play pleiotropic and cell specific roles[18,19]. Considering myeloid suppressor cells, one of our primary assumptions was that these immune-modulating cells might play a role in control of colitis, since tofacitinib facilitates the expansion of MDSCs and ameliorates experimental arthritis as well as interstitial lung disease in SKG mice[20,21]. In line with that paper, GR1 + CD11b + MDSCs were also expanded in Rag2−/− mice during early treatment with tofactinib in our hands, however, their numbers did not affect disease outcome. The data on MDSCs in inflammatory bowel disease are conflicting. Haile et al. as well as Zhang et al. described and anti-inflammatory phenotype of MDSCs[22,23] while Guan et al. as well as a recent paper from de Cicco described pro-inflammatory properties depending on the disease model[24,25]. Therefore the effect of MDSCs in disease control remain uncertain. Macrophage differentiation is affected by tofacitinib[8] suggesting a switch from M1 to M2 type macrophages. Strikingly, and comparable to our data, DSS-colitis development was not prevented in that study, but treatment was effective as soon as signs of disease developed in a rescue model of DSS colitis.

Summing up, tofacitinib is effective in the treatment of experimental CD4+ T cell transfer colitis in mice while it does not prevent occurrence of colitis. Thus time-point of treatment plays a significant role.

Methods

Mice strains

Experiments were performed with 8–12 week old C57BL/6 mice. RAG−/− (C57BL/6 J) mice were provided by A. Schippers. We used mixed genders. All mice were bred in our animal facility and kept under standardized conditions. All methods used in mice were carried out in accordance with ARRIVE guidelines.

Cell isolation

Single cell suspensions were isolated from spleens and erythrocytes were lysed with lysis buffer. $CD4^+CD25^+$ Treg cell isolation kits (Miltenyi) were used to isolate $CD4^+CD25^-$ cells and perform adoptive transfer colitis.

Transfer colitis

To induce transfer colitis, RAG2−/− mice were adoptively transferred with 2×10^6 $CD4^+$ $CD25^-$ T cells. Animals were sacrificed as soon as the loss of weight exceeded 10% of the initial bodyweight. Spleens and mLNs were harvested for further analysis. One part of the colon was fixed in formalin for histological scoring (caecum) and the upper part was fixed in RNAlater (Qiagen, Germany) for subsequent mRNA analysis.

For soluble Tofacitinib treatment, mice received either 0.05 mg/ml dissolved in drinking water resulting in a dosage of 10 mg/kg/day of Tofacitinib or of 0.2 mg/ml dissolved in drinking water resulting in a dosage of 40 mg/kg/day of Tofacitinib until end of experiments. We adopted this method from Frederike Berberich-Siebelt, who showed that tofacitinib is soluble and stable in drinking water and is taken up by mice to sufficient amounts (unpublished, personnel communication). A treatment scheme is shown in Supplementary Fig. 1.

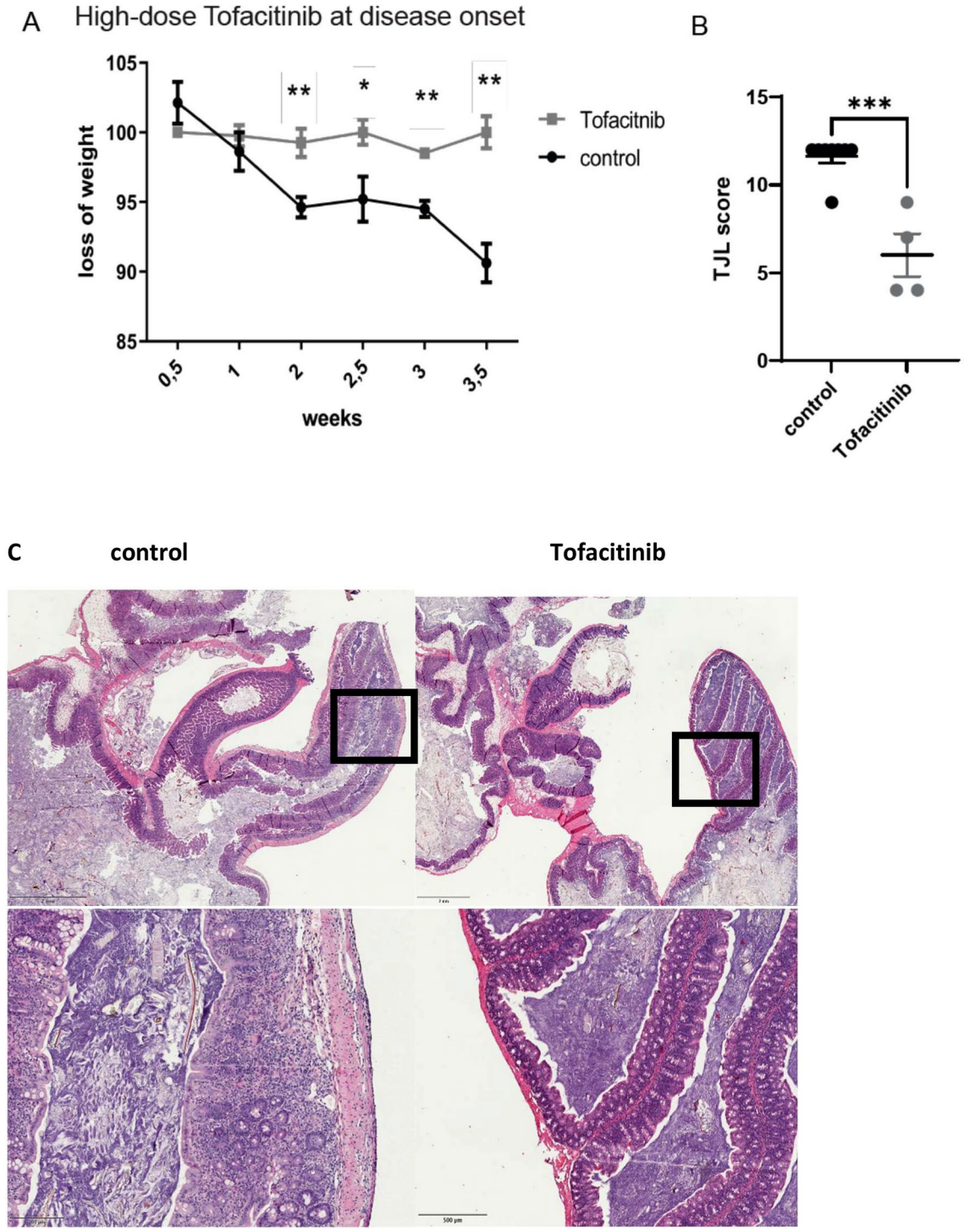


Figure 6. Tofacitinib treatment after onset of colitis reduces weight loss and intestinal inflammation. (**A**) Body weight as a percent of starting weight (N = 8 control mice, 4 Tofacitinib-treated mice, two-tailed unpaired t-tests were used, one experiment, ** = 0.0044, * = 0.0482, ** = 0.0011, ** = 0.0014). (**B**) Results of histological TJL (The Jackson Laboratory Score) scoring of colon sections. (**C**) Representative histology of colon tissue (left: control, right: tofactinib).

Histological scoring

4 µm paraffin sections from the fixed colon (caecum and proximal part) were cut serially, mounted onto glass slides, and deparaffinized. The colon sections were stained with hematoxylin and eosin by the Core Facility (IZKF) of the RWTH Aachen University. Blinded histological scoring was performed using a standard microscope, based on TJL method as described previously[26]. Each colon section was scored for the four general criteria: severity, degree of hyperplasia, degree of ulceration, if present, and percentage of area involved. A subjective

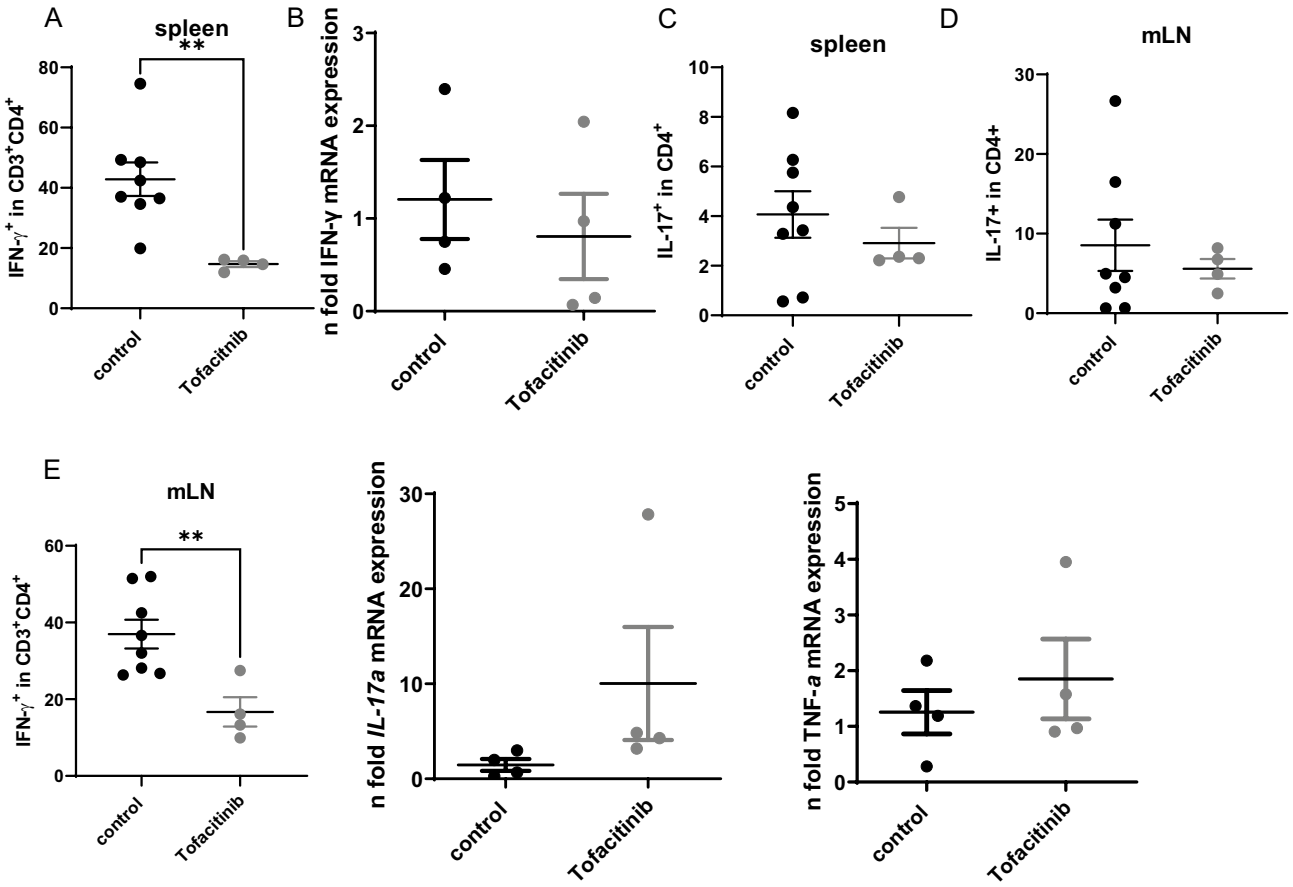


Figure 7. Tofacitinib treatment after onset of colitis reduces IFN-γ secretion. (**A**) Statistical analysis of IFN-γ+ T cells within the spleen, (N = 8 control mice and N = 4 Tofacitinib treated mice, ** = 0.0060)). (**B**) Statistical analysis of IFN-γ+ T cells within mLNs, (N = 8 control mice and N = 4 Tofacitinib treated mice, ** = 0.0070). (**C**) Statistical analysis of IL-17+ T cells within the spleen, (N = 8 control mice and N = 4 Tofacitinib treated mice). (**D**) Statistical analysis of IL-17+ T cells within mLNs, (N = 8 control mice and N = 4 Tofacitinib treated mice. (**E**) Expression of inflammatory cytokines analyzed by RT-qPCR, N = 4 c mice in each group. For A-C, error bars indicate SEM, two-tailed unpaired t-tests were used to test for significance.

range of 1–3 (1 = mild, 2 = moderate, 3 = severe) was used for the first three categories. Severity: Focally small or widely separated multifocal areas of inflammation limited to the lamina propria were graded as mild lesions (1). Multifocal or locally extensive areas of inflammation extending to the submucosa were graded as moderate lesions (2). If the inflammation extended to all layers of the intestinal wall or the entire intestinal epithelium was destroyed, lesions were graded as severe (3). Hyperplasia: Mild hyperplasia consisted of morphologically normal epithelial lining that was at least twice as thick (length of crypts) as adjacent or control mucosa. Moderate hyperplasia was characterized by the epithelial lining being two- or three-times normal thickness, cells were hyperchromatic, numbers of goblet cells were decreased, and scattered individual crypts developed an arborizing pattern. Severe hyperplastic regions exhibited markedly thickened epithelium (four or more times normal thickness), marked hyperchromasia of cells, few to no goblet cells, a high mitotic index of cells within the crypts, and numerous crypts with arborizing pattern. Ulceration was graded as: 0 = no ulcer, 1 = 1–2 ulcers (involving up to a total of 20 crypts), 2 = 1–4 ulcers (involving a total of 20–40 crypts), and 3 = any ulcers exceeding the former in size. A 10% scale was used to estimate the area involved in the inflammatory process. 0 = 0%, 1 = 10–30%, 2 = 40–70%, 3 = > 70%.

Flow cytometry

For surface staining, single cell suspensions were stained with anti-CD4, anti-CD3, (from Invitrogen and eBioscience, Germany). For intracellular staining of Foxp3, cells were fixed and permeabilized with a FOXP3 staining buffer set (eBioscience, Germany) following the manufacturer's instructions and stained with respective antibodies (Invitrogen) for 30 min. Intracellular cytokines were stained with anti- IFN-γ APC (Invitrogen) and anti-IL-17-Alexa 488 (BD), after PMA (30 nM) and Ionomycin (1.5 μM) (both Sigma-Aldrich, USA) restimulation in the presence of Golgi Plug for 5 h (antibodies see Table 1). Representative gating strategies and dot plots are shown in Supp Fig. 2.

Antibody	Lot Number	Company	Clone
CD11b Pacific Blue	4329941	Invitrogen	M1/70
Gr1 FITC	2233545	BD Biosciences	1 A8
CD3 APC	2293305	Invitrogen	145-2C11
CD4 PE	E01009-1635	eBioscience	GK1.5
CD4 Pacific Blue	2261418	Invitrogen	RM4-5
IFN-γ APC	2011141	Invitrogen	XMG1.2
IL-17 Alexa 488	7096813	BD Biosciences	TC11-18H10
CD25 Pacific Blue	2055195	Invitrogen	PC61.5
Foxp3 FITC	2152040	Invitrogen	FJK-16 s

Table 1. Antibodies used in the experiments.

Gene	Forward primer (5′→3′)	Reverse primer (5′→3′)
IFN-γ	TGCCAAGTTTGAGGTCAACAACCCA	CCCACCCCGAATCAGCAGCG
IL-17A	AGCTGGACCACCACATGAATT	CCACACCCACCAGCATCTTC
TNF-α	AGAAACACAAGATCCTGGGACAGT	CCTTTGCAGAACTCAGGAATGG

Table 2. Sequences of primers used for RT PCR.

RNA isolation and quantitative real-time PCR

Total RNA from colon tissue (distal part and sigma) was isolated using the RNeasy Mini Kit (Qiagen, Germany). cDNA was then generated from 200 ng total RNA using the RevertAid H Minus First Strand cDNA Synthesis Kit (Thermo Fisher Scientific, USA) according to the manufacturer's instructions. RT-PCR was performed using the SYBR Green PCR kit (Eurogentec, Germany) and data were acquired with the ABI prism 7300 RT-PCR system (Applied Biosystems/Life Technologies, Germany). Each measurement was set up in duplicate. After normalization to the endogenous reference control gene β-actin for mice, the relative expression was calculated (for primer sequences see Table 2).

Statistical analysis

All data are presented as mean ± standard error (SEM). Differences between two groups were evaluated using two-tailed unpaired or paired (if indicated), Student's t-test. All statistical analysis and subsequent graphics generation were performed using GraphPad Prism version 9.0 (GraphPad Software, USA). A p value < 0.05 was statistically significant.

Study approval

The study was approved by the regional government authorities and animal procedures were performed according to German legislation for animal protection. Permission for the projects was granted by the Regierungspräsident/LANUV Nordrhein-Westfalen.

Data availability

All data generated or analysed during this study are included in this paper and in the supplementary information files.

Received: 16 May 2022; Accepted: 27 February 2023
Published online: 07 March 2023

References

1. de Souza, H. S. & Fiocchi, C. Immunopathogenesis of IBD: Current state of the art. *Nat. Rev. Gastroenterol. Hepatol.* **13**, 13–27. https://doi.org/10.1038/nrgastro.2015.186 (2016).
2. Axelrad, J. E., Lichtiger, S. & Yajnik, V. Inflammatory bowel disease and cancer: The role of inflammation, immunosuppression, and cancer treatment. *World J. Gastroenterol.* **22**, 4794–4801. https://doi.org/10.3748/wjg.v22.i20.4794 (2016).
3. Ghoreschi, K. *et al.* Modulation of innate and adaptive immune responses by tofacitinib (CP-690,550). *J. Immunol.* **186**, 4234–4243. https://doi.org/10.4049/jimmunol.1003668 (2011).
4. Ghoreschi, K., Laurence, A. & O'Shea, J. J. Janus kinases in immune cell signaling. *Immunol. Rev.* **228**, 273–287. https://doi.org/10.1111/j.1600-065X.2008.00754.x (2009).
5. O'Shea, J. J., Pesu, M., Borie, D. C. & Changelian, P. S. A new modality for immunosuppression: Targeting the JAK/STAT pathway. *Nat. Rev. Drug Discov.* **3**, 555–564. https://doi.org/10.1038/nrd1441 (2004).
6. Texler, B. *et al.* Tofacitinib-induced modulation of intestinal adaptive and innate immunity and factors driving cellular and systemic pharmacokinetics. *Cell Mol. Gastroenterol. Hepatol.* **13**, 383–404. https://doi.org/10.1016/j.jcmgh.2021.09.004 (2022).
7. Gerlach, K. *et al.* The JAK1/3 inhibitor tofacitinib suppresses T cell homing and activation in chronic intestinal inflammation. *J. Crohns Colitis* https://doi.org/10.1093/ecco-jcc/jjaa162 (2020).

8. De Vries, L. C. S. *et al.* A JAK1 selective kinase inhibitor and tofacitinib affect macrophage activation and function. *Inflamm. Bowel. Dis.* **25**, 647–660. https://doi.org/10.1093/ibd/izy364 (2019).
9. Acharya, S. *et al.* Amelioration of Experimental autoimmune encephalomyelitis and DSS induced colitis by NTG-A-009 through the inhibition of Th1 and Th17 cells differentiation. *Sci. Rep.* **8**, 7799. https://doi.org/10.1038/s41598-018-26088-y (2018).
10. Covington, M. *et al.* Preclinical characterization of itacitinib (INCB039110), a novel selective inhibitor of JAK1, for the treatment of inflammatory diseases. *Eur. J. Pharmacol.* **885**, 173505. https://doi.org/10.1016/j.ejphar.2020.173505 (2020).
11. Unterweger, A. L. *et al.* Suppressing Kv1.3 ion channel activity with a novel small molecule inhibitor ameliorates inflammation in a humanised mouse model of ulcerative colitis. *J. Crohns Colitis* **15**, 1943–1958. https://doi.org/10.1093/ecco-jcc/jjab078 (2021).
12. Brand, R. M. *et al.* Tofacitinib inhibits inflammatory cytokines from ulcerative colitis and healthy mucosal explants and is associated with pSTAT1/3 reduction in T-cells. *Am. J. Physiol. Gastrointest. Liver Physiol.* **320**, G396-g410. https://doi.org/10.1152/ajpgi.00383.2020 (2021).
13. Yokoyama, S. *et al.* Janus kinase inhibitor tofacitinib shows potent efficacy in a mouse model of autoimmune lymphoproliferative syndrome (ALPS). *J. Clin. Immunol.* **35**, 661–667. https://doi.org/10.1007/s10875-015-0203-z (2015).
14. Park, H. B. *et al.* CP-690550, a Janus kinase inhibitor, suppresses CD4+ T-cell-mediated acute graft-versus-host disease by inhibiting the interferon-γ pathway. *Transplantation* **90**, 825–835. https://doi.org/10.1097/TP.0b013e3181f24e59 (2010).
15. Reddig, A. *et al.* Impact of different JAK inhibitors and methotrexate on lymphocyte proliferation and DNA damage. *J. Clin. Med.* https://doi.org/10.3390/jcm10071431 (2021).
16. van Vollenhoven, R. *et al.* Evaluation of the short-, mid-, and long-term effects of tofacitinib on lymphocytes in patients with rheumatoid arthritis. *Arthritis Rheumatol.* **71**, 685–695. https://doi.org/10.1002/art.40780 (2019).
17. Yoshida, H. *et al.* Low dose CP-690,550 (tofacitinib), a pan-JAK inhibitor, accelerates the onset of experimental autoimmune encephalomyelitis by potentiating Th17 differentiation. *Biochem. Biophys. Res. Commun.* **418**, 234–240. https://doi.org/10.1016/j.bbrc.2011.12.156 (2012).
18. Cordes, F. *et al.* Tofacitinib reprograms human monocytes of ibd patients and healthy controls toward a more regulatory phenotype. *Inflamm. Bowel. Dis.* **26**, 391–406. https://doi.org/10.1093/ibd/izz213 (2020).
19. Cordes, F., Foell, D., Ding, J. N., Varga, G. & Bettenworth, D. Differential regulation of JAK/STAT-signaling in patients with ulcerative colitis and Crohn's disease. *World J. Gastroenterol.* **26**, 4055–4075. https://doi.org/10.3748/wjg.v26.i28.4055 (2020).
20. Sendo, S., Saegusa, J., Yamada, H., Nishimura, K. & Morinobu, A. Tofacitinib facilitates the expansion of myeloid-derived suppressor cells and ameliorates interstitial lung disease in SKG mice. *Arthritis Res. Ther.* **21**, 184. https://doi.org/10.1186/s13075-019-1963-2 (2019).
21. Nishimura, K. *et al.* Tofacitinib facilitates the expansion of myeloid-derived suppressor cells and ameliorates arthritis in SKG mice. *Arthritis Rheumatol.* **67**, 893–902. https://doi.org/10.1002/art.39007 (2015).
22. Haile, L. A. *et al.* Myeloid-derived suppressor cells in inflammatory bowel disease: A new immunoregulatory pathway. *Gastroenterology* **135**(871–881), 881.e871–875. https://doi.org/10.1053/j.gastro.2008.06.032 (2008).
23. Zhang, J. *et al.* Protein tyrosine phosphatase 1B deficiency ameliorates murine experimental colitis via the expansion of myeloid-derived suppressor cells. *PLoS ONE* **8**, e70828. https://doi.org/10.1371/journal.pone.0070828 (2013).
24. Guan, Q. *et al.* The role and potential therapeutic application of myeloid-derived suppressor cells in TNBS-induced colitis. *J. Leukoc. Biol.* **94**, 803–811. https://doi.org/10.1189/jlb.0113050 (2013).
25. De Cicco, P., Sanders, T., Cirino, G., Maloy, K. J. & Ianaro, A. Hydrogen sulfide reduces myeloid-derived suppressor cell-mediated inflammatory response in a model of helicobacter hepaticus-induced colitis. *Front. Immunol.* **9**, 499. https://doi.org/10.3389/fimmu.2018.00499 (2018).
26. Mähler, M. *et al.* Genetic analysis of susceptibility to dextran sulfate sodium-induced colitis in mice. *Genomics* **55**(2), 147–56 (1999).

Acknowledgements
The study was supported by a competitive grant program from Pfizer. Frederike Berberich Siebelt shared the unpublished protocol on Tofictinib treatment in drinking water.

Author contributions
S.H.S.: performed experiments, analyzed data, and wrote the manuscript, J.T.H.: performed experiments, K.O.: performed experiments, analyzed data, and revised the manuscript, A.P.: analyzed the data and reviewed the manuscript, A.S.: analyzed data and reviewed the manuscript, N.W.: reviewed the manuscript, K.T.: designed the study, analyzed data, and revised the manuscript.

Funding
Open Access funding enabled and organized by Projekt DEAL.

Competing interests
The authors declare no competing interests.

Additional information
Supplementary Information The online version contains supplementary material available at https://doi.org/10.1038/s41598-023-30616-w.

Correspondence and requests for materials should be addressed to K.T.

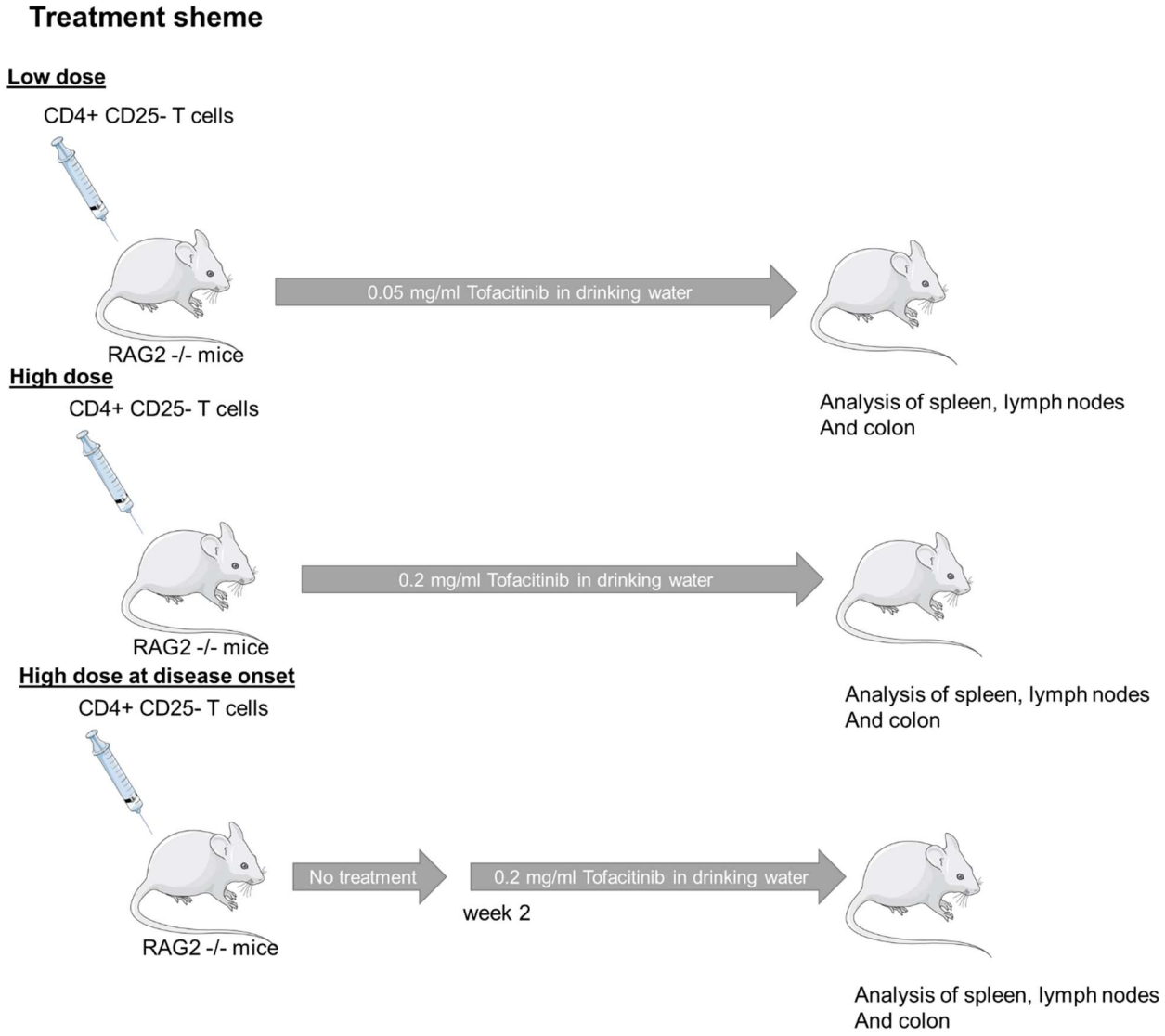
Reprints and permissions information is available at www.nature.com/reprints.

Publisher's note Springer Nature remains neutral with regard to jurisdictional claims in published maps and institutional affiliations.

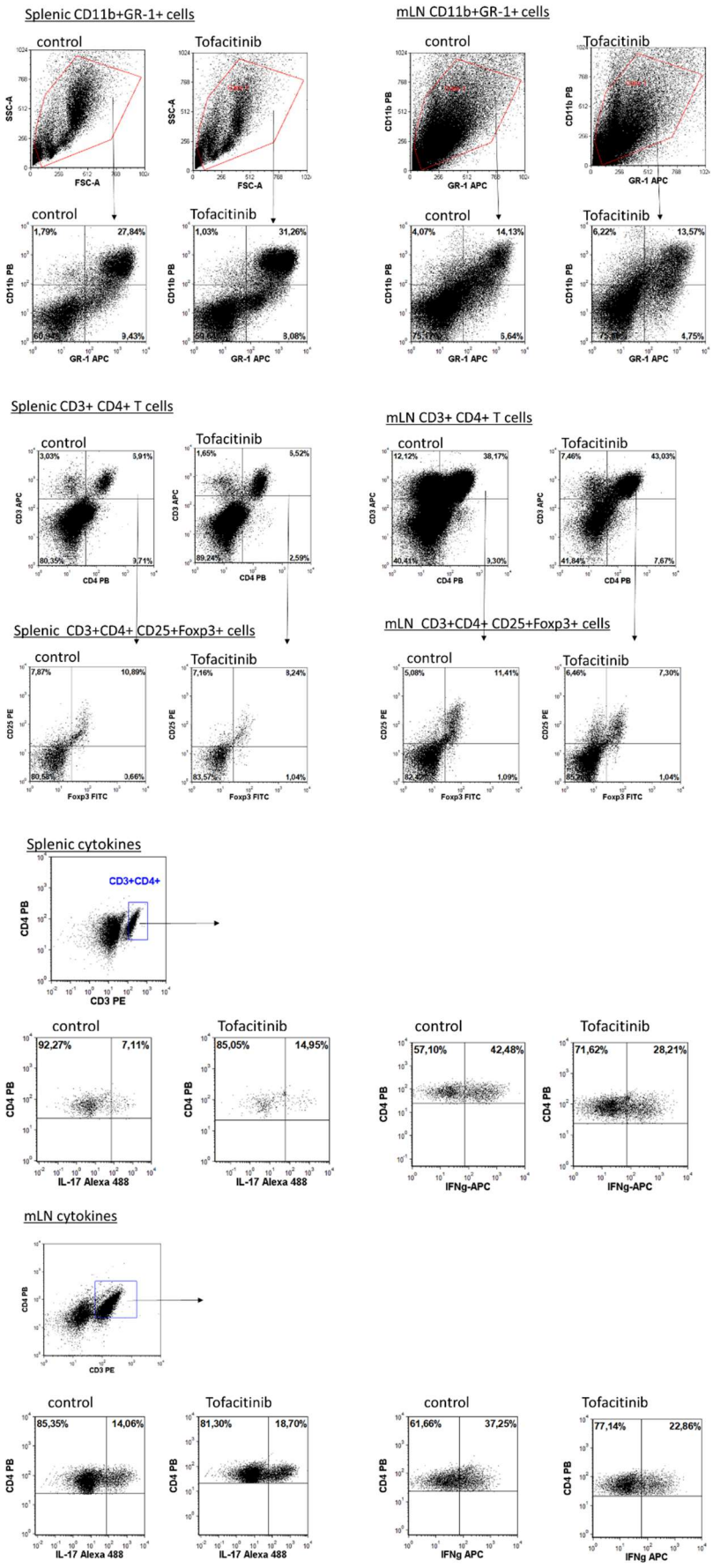
Open Access This article is licensed under a Creative Commons Attribution 4.0 International License, which permits use, sharing, adaptation, distribution and reproduction in any medium or format, as long as you give appropriate credit to the original author(s) and the source, provide a link to the Creative Commons licence, and indicate if changes were made. The images or other third party material in this article are included in the article's Creative Commons licence, unless indicated otherwise in a credit line to the material. If material is not included in the article's Creative Commons licence and your intended use is not permitted by statutory regulation or exceeds the permitted use, you will need to obtain permission directly from the copyright holder. To view a copy of this licence, visit http://creativecommons.org/licenses/by/4.0/.

© The Author(s) 2023, corrected publication 2025

Supplemental Figures



Suppl. Fig. 1: Treatment scheme



Suppl. Fig. 2: Gating strategies and representative Dot plots.

Acknowledgements

I wish to express my deepest gratitude to my supervisor, Prof. Dr. med. Klaus Tenbrock, for his outstanding guidance, continuous support, and constructive criticism throughout the course of my doctoral research. His profound scientific expertise, critical perspective, and dedication to excellence have greatly influenced not only the quality of this dissertation but also my overall academic development. I am indebted to him for his constant encouragement, insightful discussions, and generous investment of time, which have been fundamental in shaping both my research and my professional growth.

I am equally indebted to my co-supervisor, Dr. rer. nat. Kim Ohl, for her invaluable advice, encouragement, and thoughtful feedback. Her sound guidance, openness to dialogue, and keen observations provided clarity at crucial moments and made substantial contributions to the advancement of this work.

I am sincerely grateful to Judit for her generous assistance, remarkable patience and her consistent support in the laboratory proved indispensable for the successful completion of several experimental procedures.

I also extend my thanks to my colleagues, Chris, Renske, Anandhi and others, for their active collaboration, insightful exchanges of ideas, and for fostering a collegial and intellectually stimulating research environment. Their contributions, both on a professional and interpersonal level, have made my time in the laboratory not only productive but also motivating and rewarding.

I would also like to express my sincere thanks to all cooperation partners, whose generous support, valuable guidance, and collaborative spirit greatly contributed to the success of this work.

My heartfelt gratitude is owed to my parents, whose unwavering belief in my abilities and enduring support have accompanied me throughout my academic journey. Their sacrifices, dedication, and encouragement provided me with the strength to persevere in challenging times and pursue my scholarly goals with determination.

Above all, I am profoundly indebted to my wife, Zhou, and my children, Pradhi and Priya, for their patience, understanding, and unconditional support. Their encouragement during the demanding phases of this research, combined with their love and belief in me, has been a constant source of motivation and resilience. This work would not have been possible without their steadfast presence and the balance they provided between personal life and academic commitments.

Affidavit according to § 5 (1) for Data Retention

Hiermit erkläre ich, dass die dieser Dissertation zu Grunde liegenden Originaldaten (I hereby declare that the original data forming the basis of this doctoral thesis are stored)

im Klinik für Kinder- und Jugendmedizin, Uniklinik RWTH Aachen, Pauwelstraße 30, Aachen

hinterlegt sind.

Affidavit according to § 5 (1) and (2), and § 11 (3) 12 of the doctoral studies regulations

I, **Sudheendra Hebbar Subramanyam,** hereby declare on oath, that I have contributed a significant part, and thus majority, of the publication:
Hebbar Subramanyam S, Turyne Hriczko J, Schulz S, Look T, Goodarzi T, Clarner T, Scheld M, Kipp M, Verjans E, Böll S, Neullens C, Costa I, Li Z, Gan L, Denecke B, Schippers A, Floess S, Huehn J, Schmitt E, Bopp T, Wasmuth H, Winograd R, Beyaert R, Lambrecht B, Zenke M, Wagner N, Ohl K, Tenbrock K. CREB regulates Foxp3+ST-2+ TREGS with enhanced IL-10 production. Front in Immunology. 2025 Jul 24;16:1601008.

The contributions to the publication were as follows:

	S. Hebbar Subramanyam	J Turyne Hriczko	S. Schulz	T. Look	T.Goodarzi	T. Clarner	M.Scheld	E. Verjans	S. Boell	C. Neullens	S. Floess	I. Costa	Z. Li	L. Gan	B. Denecke	J. Huehn	M. Zenke	K. Ohl	K. Tenbrock	Sum (%)
Investigation	60	2	2	2	2	3	3	2	2	2	4							16		100
Formal Analysis	60										3	3	3	3	3	3	3	19		100
Visualization	60																	20	20	100
Methodology	40																	30	30	100
Writing/draft of the manuscript	**100**																			100
Reviewing of the manuscript (continued in next page)		2	2	2	2	2	2	2	2	2	2	2	2	2	2	2	2	25	25	82

The position as the first author obviously arises from this significant contribution.

Sudheendra Hebbar Subramanyam

As supervisor and / or corresponding author I confirm the statements of Sudheendra Hebbar Subramanyam and as a representative of the collaborative partners and non-reachable co-authors [B. Denecke]

Klaus Tenbrock
As co-author I endorse the statement of Klaus Tenbrock

J. Turyne Hriczko	S. Schulz	T. Look	T. Goodarzi
T. Clarner	M. Scheld	E. Verjans	S. Boell
C. Neullens	S. Floess	I. Costa	Z. Li
L. Gan	J. Heuhn	M. Zenke	K. Ohl

Affidavit according to § 5 (1) and (2), and § 11 (3) 12 of the doctoral studies regulations

I, **Sudheendra Hebbar Subramanyam,** hereby declare on oath, that I have contributed a significant part, and thus majority, of the publication:
Hebbar Subramanyam S, Turyne Hriczko J, Schulz S, Look T, Goodarzi T, Clarner T, Scheld M, Kipp M, Verjans E, Böll S, Neullens C, Costa I, Li Z, Gan L, Denecke B, Schippers A, Floess S, Huehn J, Schmitt E, Bopp T, Wasmuth H, Winograd R, Beyaert R, Lambrecht B, Zenke M, Wagner N, Ohl K, Tenbrock K. CREB regulates Foxp3+ST-2+ TREGS with enhanced IL-10 production. Front in Immunology. 2025 Jul 24;16:1601008.
The contributions to the publication were as follows:

	A. Schippers	M. Kipp	T.Bopp	E. Schmitt	H. Wasmuth	R. Winograd	R. Bayeart	B. Lambrecht	J. Huehn	M. Zenke	N. Wagner	K. Ohl	K. Tenbrock	Sum (%)
Funding													100	100
Supervision												40	60	100
Conceptualization		9	9						9	9		24	40	100
Resources	25		10	10	5	5	10	10			25			100
Data Curation												40	60	100
Project Administration												50	50	100
Reviewing of the manuscript	2	2	2	2	2	2	2	2			2			100

The position as the first author obviously arises from this significant contribution.

Sudheendra Hebbar Subramanyam

As supervisor and / or corresponding author I confirm the statements of Sudheendra Hebbar Subramanyam and as a representative of the non-reachable co-authors

Klaus Tenbrock

As co-author I endorse the statement of Klaus Tenbrock

A. Schippers	T. Bopp	E. Schmitt	H. Wasmuth
R. Winograd	R. Bayeart	B. Lambrecht	J. Heuhn
M. Zenke	N. Wagner	M. Kipp	K. Ohl

Affidavit according to § 5 (1) and (2), and § 11 (3) 12 of the doctoral studies regulations

I, **Sudheendra Hebbar Subramanyam,** hereby declare on oath, that I have contributed a significant part, and thus majority, of the publication:
Subramanyam SH, Hriczko JT, Pappas A, Schippers A, Wagner N, Ohl K, Tenbrock K. Tofacitinib fails to prevent T cell transfer colitis in mice but ameliorates disease activity. Sci Rep. 2023 Mar 7;13(1):3762.

The contributions to the publication were as follows:

	S. Hebbar Subramanyam	J. Turyne Hriczko	A. Pappa	A. Schippers	N. Wagner	K. Ohl	K. Tenbrock	Sum %
Funding acquisition							100	100
Supervision						30	70	100
Conceptualization							100	100
Investigation	70	10				20		100
Visualization	60					30	10	100
Formal analysis	60		5	5		15	15	100
Methodology	40					30	30	100
Resources				50	50			100
Data curation						40	60	100
Project administration						40	60	100
Writing of original draft	**100**							100
Review/Revise of draft			10	10	10	30	40	100

The position as the first author obviously arises from this significant contribution.

Sudheendra Hebbar Subramanyam

As supervisor and / or corresponding author I confirm the statements of Sudheendra Hebbar Subramanyam and as a representative of the collaborative partners

Klaus Tenbrock

As co-author I endorse the statement of Klaus Tenbrock

J. Turyne Hriczko | A. Pappa | A. Schippers | N. Wagner

K. Ohl